NATIONAL ADVISORY COMMITTEE FOR AERONAUTICS

WARTIME REPORT

ORIGINALLY ISSUED
March 1942 as
Advance Restricted Report

CHARACTERISTICS OF PLAIN AND BALANCED ELEVATORS ON A TYPICAL PURSUIT FUSELAGE AT ATTITUDES SIMULATING NORMAL-FLIGHT AND SPIN CONDITIONS

By Richard I. Sears and H. Page Hoggard, Jr.

Langley Memorial Aeronautical Laboratory
Langley Field, Va.

NACA

WASHINGTON

NATIONAL ADVISORY COMMITTEE FOR AERONAUTICS

ADVANCE RESTRICTED REPORT

CHARACTERISTICS OF PLAIN AND BALANCED ELEVATORS ON A TYPICAL PURSUIT FUSELAGE AT ATTITUDES SIMULATING NORMAL-FLIGHT AND SPIN CONDITIONS

By Richard I. Sears and H. Page Hoggard, Jr.

SUMMARY

Lift and elevator hinge-moment characteristics of a horizontal tail, provided with various plain and balanced elevators and mounted on a typical pursuit fuselage, were measured in the NACA 7- by 10-foot wind tunnel at attitudes simulating normal-flight and spin conditions.

The lift effectiveness of the elevator was practically independent of the size of the aerodynamic balance. The elevator with a large overhang was overbalanced throughout some range of deflections and would therefore require the use of an unbalancing tab for satisfactory operation. Because, at angles of attack above the airfoil stall, the elevator maintained about half of its lift effectiveness, increments of lift can be obtained to upset the spin equilibrium and effect a recovery if the elevator can be moved. The plain unbalanced elevator generally floated at lower negative deflections than did the balanced elevator under spin condition. A trimming tab, deflected in the same direction as the elevator, presents a feasible means of reducing the stick forces in a spin to a magnitude the pilot is capable of exerting.

INTRODUCTION

Because the trend of design of modern aircraft is toward airplanes of high speed and large size, it has become increasingly necessary to reduce the hinge moments of the control surfaces so that, for all conditions of flight, the control-stick forces are of a magnitude the pilot is capable of applying. The reduction of control-surface hinge moments must be accomplished in such a manner as to improve and not to impair the flying qualities of the airplane. In an effort to solve this problem, the NACA is conducting an extensive investigation of the aerodynamic characteristics of control surfaces. The main objectives of this investigation are to arrive at a rational method for designing airplane control surfaces, to

determine the type of flap arrangements best suited for use as a control surface, and to supply experimental data for design purposes.

The fundamental part of the NACA investigation is being made in two-dimensional flow. Reference 1 presents some theoretical consideration for airfoils with flaps and some experimentally determined design parameters for plain flaps of any chord. The effect of gap at the nose of a plain flap is given in reference 2. Section characteristics of a flap with a large, a small, and a medium aerodynamic balance of various nose shapes are reported in references 3, 4, and 5, respectively.

Certain modern airplanes have such excessive stick forces in a spin that the pilot is unable to move the controls to make a recovery. One purpose of the present investigation was, therefore, to provide data on the aerodynamic characteristics of elevators at attitudes simulating spin conditions. This investigation was also undertaken to provide experimental data on finite span, balanced control surfaces, and to help establish a correlation between the characteristics in two-dimensional and three-dimensional flow.

SYMBOLS AND DEFINITIONS

The symbols used in this paper are:

C_L lift coefficient (L/qS)

C_D drag coefficient (D/qS)

C_h elevator hinge-moment coefficient $(H/q\bar{c}_eS_e)$

where

L lift of fuselage-tail combination

D drag of fuselage-tail combination

H elevator hinge moment

q dynamic pressure

S horizontail tail area

S_e	elevator area
c	mean geometric chord of tail
c_e	mean geometric chord of elevator
c_t	mean geometric chord of tab
$\overline{c}_e$	root-mean-square chord of elevator

and

α	angle of attack of tail surface
ψ	angle of yaw
δ_e	elevator deflection with respect to stabilizer (positive with trailing edge deflected downward)
δ_t	tab deflection with respect to elevator (positive with trailing edge deflected downward)
A	aspect ratio

also

$$C_{L_\alpha} = \left(\frac{\partial C_L}{\partial \alpha}\right)_\delta$$

$$C_{L_\delta} = \left(\frac{\partial C_L}{\partial \delta}\right)_\alpha$$

$$C_{h_\alpha} = \left(\frac{\partial C_h}{\partial \alpha}\right)_\delta$$

$$C_{h_\delta} = \left(\frac{\partial C_h}{\partial \delta}\right)_\alpha$$

etc.

Lower-case letters are used to indicate section coefficients determined in the two-dimensional-flow investigations of references 1, 2, 3, 4, and 5. The subscript indicates the factor held constant in determining the parameter.

Certain terms as used in this paper are defined or explained as follows:

1. The terms "flap," "control surface," and "elevator" are used synonymously.

2. The terms "overhang" and "balance" are used synonymously.

3. An "unbalanced" flap is a plain flap with a nose radius approximately equal to the semithickness of the airfoil section at the hinge axis.

4. The elevator chord is measured from the hinge axis to the trailing edge of the airfoil.

5. The overhang is measured from the hinge axis to the nose of the movable surface.

APPARATUS AND MODEL

The tests were made in the NACA 7- by 10-foot wind tunnel described in references 6 and 7. The model was mounted in the conventional manner on the balance fork for force-test measurements. The elevator hinge moments were measured electrically by a calibrated torque rod located inside the fuselage of the model.

The plan form of the horizontal tail tested is shown in figure 1. It had the following physical characteristics:

NACA 0009 airfoil section

$S_e/S = 0.27$

S = 257 square inches (including the area projected through the fuselage)

A = 3.7

Taper ratio = 1.77:1

c = 8.245 inches

c_e = 2.27 inches

$\bar{c}_e$ = 2.39 inches

c_t = 0.20 c_e

The tail surface was provided with interchangeable blocks to give the following five arrangements of balance (fig. 1):

1. Unbalanced flap with blunt nose

2. $0.35c_e$ balance with blunt nose

3. $0.35c_e$ balance with sharp nose

4. $0.50c_e$ balance with blunt nose

5. $0.50c_e$ balance with sharp nose

The horizontal tail surface was mounted on a model of a typical pursuit fuselage (fig. 2) at an angle of incidence of 2.3°. The fuselage juncture was filleted. The model had no wing, propeller, or vertical tail. The cutout for the wing through the fuselage was faired in.

The elevator deflections were held by a friction clamp on the torque rod. Tab deflections were held by the stiffness of bent brass wire hinges. All deflections were set by templets.

TESTS

The tests were made at a dynamic pressure of 16.37 pounds per square foot, which corresponds to a velocity of 80 miles per hour under standard sea-level conditions. Based on the average chord of the horizontal tail, the test Reynolds number was 502,000. The effective Reynolds number of the tests was 803,000, the turbulence factor of the 7- by 10-foot atmospheric tunnel being 1.6.

In order to simulate spin as well as normal-flight conditions, the model was tested throughout an angle-of-attack range from about -10° to 47° and through a yaw range from about -10° to 45°. Two gap variations, sealed and 0.005c gap, were investigated.

At 0° angle of yaw, the model was tested throughout the angle-of-attack range at elevator deflections of 5°, 0°, -10°, -20°, and -30° for the unbalanced elevator and at 5°, 0°, -10°, -15°, and -20° for the balanced elevators. With an unsealed gap, tests were made at each elevator de-

flection with the tab neutral; but, with a sealed gap, the tab was deflected -10°, 0°, 10° for each elevator deflection. Readings were taken at 4° increments of angle of attack in the unstalled range, at 1° increments during the transition from the unstalled to the stalled state, and at 5° increments in the range where the tail surface was completely stalled.

All tests throughout the yaw range were made with a sealed gap and with tab neutral. In order to simulate yawed flight at unstalled attitudes, all elevators were tested throughout the yaw range at 2.3° and 14.3° angle of attack of the tail with 5°, 0°, and -10° elevator deflections. In order to simulate conditions encountered in a spin, all elevators were tested throughout the yaw range at 27.3° and 47.3° angle of attack with large elevator deflections. The unbalanced elevator was deflected -20° and -30° and the balanced elevators -15° and -20° for these tests. Readings were taken at 5° increments of angle of yaw throughout the yaw range.

The gap between the stabilizer and the elevator was 0.005c when unsealed. Sealing the gap was accomplished by filling it with a light grease. All tests were made with the tab gap sealed.

Tests were made of the fuselage alone throughout the angle-of-attack range at 0° yaw and throughout the yaw range at 0°, 12°, 25°, and 45° angle of attack of the fuselage. Because of the 2.3° angle of incidence, the angle of attack of the fuselage equals the angle of attack of the tail minus 2.3°.

PRECISION

Because of the small size of the tail surface tested, no corrections were necessary for the effect of the tunnel walls. Strut-interference effects have also been neglected.

The angles of attack were set to within $\pm0.1^\circ$ and the surface deflections to within $\pm0.2^\circ$. Values of lift and drag coefficients were measured to within ±0.002 and values of elevator hinge-moment coefficients to within ±0.003. The differences in drag of the various elevators when neutral were not measurable; it was less than 0.002.

PRESENTATION OF DATA

Because a primary purpose of these tests is to furnish data on finite balanced control surfaces, lift and hinge-moment characteristics as affected by angle of attack, angle of yaw, elevator deflection, tab deflections, and elevator gap are presented for each of the five elevators tested. Because the various tails were mounted on a fuselage, all the characteristics presented include the mutual-interference effects of the fuselage and the horizontal tail.

The characteristics of the fuselage alone are presented in figure 3 as a function of angle of attack at 0° yaw and as a function of angle of yaw at four angles of attack.

The lift coefficients of the various fuselage-tail combinations and the corresponding elevator hinge-moment coefficients are presented in figures 4 to 8 as a function of angle of attack of the tail for several elevator deflections with zero tab deflection. Part (a) of each figure presents these characteristics with the elevator gap sealed with grease, and part (b) presents the data with this gap equal to 0.005c.

The increments of lift coefficient ΔC_L of the tail surface alone plus interference and the corresponding increment of elevator hinge-moment coefficient ΔC_h caused by angle of yaw are presented as a function of angle of yaw in figures 9 to 13 for each of the tails. These increments were found by deducting the characteristics of the tail plus interference in the unyawed condition from the characteristics of the yawed condition, all other factors being constant. The lift of the tail alone plus interference was found by deducting the lift of the fuselage alone from that of the fuselage-tail combination at the same attitude. Parts (a), (b), (c), and (d) of figures 9 to 13 give the data plotted as a function of angle of yaw for a different angle of attack and for several elevator deflections. The elevator-stabilizer gap was sealed and the tab was neutral for the data presented in these figures.

The increment of lift coefficient of the fuselage-tail combinations and the corresponding increment of elevator hinge-moment coefficient caused by 10° and -10° tab

deflections are presented as a function of both angle of attack and elevator deflection in figures 14 to 18 for each of the five tails. These increments were found by deducting characteristics of the model with tab neutral from characteristics with the tab deflected, all other factors being constant. Part (a) of figures 14 to 18 gives the coefficient increments due to tab deflection as a function of angle of attack at zero elevator deflection and zero yaw. Parts (b) and (c) of these figures give the coefficient increments due to tab deflection as a function of elevator deflection at several angles of attack and zero yaw. The data presented in these figures were obtained with the elevator gap sealed with grease.

The angle-of-attack of the tail used for presenting some of the data of figures 9 to 18 were chosen to represent:

1. A small unstalled angle of attack, 2.3°
2. A large unstalled angle of attack, 14.3°
3. An angle of attack slightly above the stall, 27.3°
4. An angle of attack far above the stall, 47.3°

Characteristics are presented in these figures for small elevator deflections at the unstalled angles of attack and for large elevator deflections at the stalled angles of attack in order to approximate flight conditions.

DISCUSSION

Fuselage Alone and Fuselage Interference

The lift of the fuselage alone is shown in figure 3 to be negligible; $C_{L_\alpha} = 0.0003$ at angles of attack below that at which the tail stalls. At an angle of attack of 20°, C_{L_α} becomes 0.003 and the lift coefficient C_L, based on tail-surface dimensions, increases gradually and steadily to a maximum value of 0.009, at the largest angle of attack tested.

Because of fuselage interference, the angle of attack of zero lift for all the tails (figs. 4 to 8) was

about 1°. This interference effect agrees qualitatively with previous experimental data.

The slopes of all the curves of figures 4 to 8 are affected somewhat by an unknown interference factor. The slope of the lift curves in the unstalled range is very nearly that of the tail alone plus interference because the contribution to lift by the fuselage alone has already been shown to be negligible in this range. Above the stall, however, some of the increase in lift with angle of attack may be attributed to the fuselage (fig. 3).

As the fuselage is yawed at small angles of attack (fig. 3(b), $\alpha = 2.5^\circ$), the lift of the fuselage increases positively. At larger angles of attack, however, the lift decreases with angle of yaw. Consequently, a large part of the increment of lift of the fuselage-tail combination due to yaw is caused by the fuselage itself.

Lift Characteristics of Fuselage-Tail Combinations

With a sealed gap, all elevators tested showed the slope of the lift curve C_{L_α} to be 0.053 (figs. 4 to 8). With an unsealed gap of 0.005c, this slope was generally slightly less, being about 0.051 or 0.050. Above the stall, the C_L of the combination increased slightly with increasing angle of attack. In the range of angles of attack from 33° to 47°, the increment of lift coefficient of the fuselage alone was about 0.04 and that of the combination was about 0.10. The results indicate that, as the angle of attack was increased beyond the stall, the lift of the tail alone plus interference did increase slightly, as is normally characteristic of thin airfoils.

The effectiveness of the various elevators in producing lift is practically independent of the size and the shape of the aerodynamic balance. With the gap sealed, the slope C_{L_δ} was 0.029 for all blunt-nose elevators and 0.028 for sharp-nose elevators regardless of the size of overhang (figs. 4 to 8). Unsealing the gap did not change the effectiveness C_{L_δ} for elevators with a blunt-nose balance. For a plain elevator and elevators with a sharp-nose balance C_{L_δ} was about 10 percent less with an open gap than with a sealed gap. These results are in agreement with the section data of references 2 to 5.

At angles of attack beyond the stall, the lift effectiveness of all elevators is about half as great as before the stall. Elevator deflections that are ineffective in producing increments of lift below the stall become effective when the airfoil has completely stalled. (See $\delta_e = -30$ in fig. 4(a) and $\delta_e = -20$ in figs. 5(b), 6(b), 7(a), and 7(b).) Thus, if the elevator can be moved when the airplane is in spin attitudes, increments of lift can be obtained to upset the spin equilibrium and effect a recovery.

The approximate maximum deflection to which the elevator was effective in producing an increment of lift below the airfoil stall, when deflected in opposition to the angle of attack, was 30° for a plain elevator, 20° for a 0.35c balanced elevator, and 15° for a $0.50c_e$ balanced elevator. These limits for the balanced elevators are closely associated with the unporting angle of the elevator, the angle at which the nose of the balance protrudes above the stabilizer.

The plain elevator with open gap (fig 4(b)) and the $0.50c_e$ sharp-nose, balanced elevator with sealed gap (fig. 8(a)) showed nearly linear effectiveness throughout the unstalled angle-of-attack range for deflections to the limits given. With sealed gap the plain elevator (fig. 4(a)) showed nearly linear effectiveness to about 25° deflection but, at 30° deflection although the elevator had not stalled, violent separation had occurred resulting in a large loss in lift effectiveness throughout the unstalled angle-of-attack range. The $0.35c_e$ sharp-nose, balanced elevator with sealed gap (fig 6(a)), the $0.50c_e$ blunt-nose, balanced elevator with sealed gap (fig. 7(a)), and the $0.50c_e$ sharp-nose balanced elevator with sealed gap (fig. 8(a)) all gave approximately linear characteristics with elevator deflections for values below the unporting angle stated, when deflected in opposition to the angle of attack. When deflected in conjunction with the angle of attack, however, these elevators showed large losses in lift effectiveness at the limiting deflection, indicating a severe separation of flow. The $0.35c_e$ sharp-nose, balanced elevator with open gap (fig. 6(b)), the $0.35c_e$ blunt-nose, balanced elevator with both sealed and open gap (figs. 5(a) and 5(b)), and the $0.50c_e$ sharp-nose, balanced elevator with open gap (fig. 8(b)) also showed linear lift effectiveness to the deflection limits given when deflected in opposition to the angle of attack. The

elevators of this group, however, when deflected in conjunction with the angles of attack to the limits stated, produced negative lift effectiveness, indicating a stalled condition of the elevator.

Thus, when large amounts of aerodynamic balance are employed, the maximum angle to which the elevator may be deflected in conjunction with the angle of attack is less than that for a plain flap. This fact should be recognized in the design of a control surface employing a large amount of overhang.

The variation with angle of yaw of lift of the tail alone plus interference (figs. 9 to 13) was such that, at small unstalled angles of attack ($\alpha = 2.3^{\circ}$) the increment of lift coefficient ΔC_L caused by yaw was positive and increased in magnitude to 40° yaw. As the angle of yaw was increased further to 44°, ΔC_L decreased. The increment of lift due to yaw at a given angle of yaw generally became slightly more positive as the elevator was deflected upward (negatively). At 14.3° angle of attack the increment of tail lift coefficient due to yaw was negative and increased in magnitude but not linearly, as the angle of yaw was increased. At 27.3° and 47.3° angle of attack, however, the increment of tail lift coefficient remained nearly zero up to about 20° angle of yaw. As the tail was yawed farther, the increment became negative and increased in magnitude. Beyond about 39° angle of yaw, the negative increment of lift coefficient generally showed a tendency to remain constant or even to decrease in magnitude as the tail was yawed to the maximum angle tested. At 27.3° and 47.3° angle of attack, ΔC_L due to yaw was only to a slight extent dependent on elevator deflection.

The above-mentioned considerations apply generally to all five elevators tested. The degree to which each elevator fits these generalities is indicated in the curves for each elevator. (See figs. 9 to 13.) Figure 3 indicates the part of the total change in lift of the fuselage-tail combination caused by the fuselage alone as the model is yawed.

The variation of lift with yaw at 14.3° angle of attack is such as to increase negatively the lift on the tail as the airplane is yawed. This effect will tend to oppose the diving moment produced by the motion of the tail away from the region of strong downwash at the center of the wing as the complete airplane is yawed.

Lift Effectiveness of the Tab

The effectiveness of the tab in producing increments of lift was practically independent of the amount of elevator balance (figs. 14 to 18). The tab was slightly less effective in changing the lift of the horizontal tail surface with a sharp-nose, balanced elevator than with a plain elevator or a blunt-nose, balanced elevator. This result is apparent from a comparison of part (a) of figures 16 and 18 with part (a) of figures 14, 15, and 17.

The lift effectiveness of the tab for 10° and -10° deflection at zero elevator deflection was practically constant throughout the unstalled range of angles of attack. At angles of attack beyond the stall the tab on all elevators became less effective in producing increments of lift. Qualitatively this is the same result as was found for the elevator effectiveness at angles of attack beyond the stall. For all elevators the lift effectiveness of the tab deflected 10° and -10° was nearly independent of elevator deflection.

Elevator Hinge Moments

For all elevator arrangements the variation of elevator hinge-moment coefficient C_h with angle of attack and elevator deflection, as indicated in figures 4 to 8, is linear at attitudes where the air flow has not separated over the flap. When the air flow separated over the elevator, the hinge-moment coefficient curves became nonlinear and the magnitude of the coefficient increased as separation progressed. When the entire airfoil stalled at some positive angle of attack, the center of pressure on the elevator moved to the rear, giving rise to large negative increments of hinge moment. At angles of attack beyond the stall, C_{h_α} is generally negative and the curves of hinge-moment coefficient as a function of angle of attack (figs. 4 to 8) are fairly regular. At large stalled angles of attack the elevator floats freely, generally at some large negative deflection.

At unstalled angles of attack, the elevators having a $0.35c_e$ balance with either a blunt or a sharp nose (figs. 5 and 6) gave appreciable reductions in hinge-moment coefficient over a plain elevator (fig. 4). The sharp-nose balance did not give quite as small a value of C_{h_δ} as

L-379

did the blunt-nose balance, but its balancing effectiveness was maintained to higher deflections. This result is in agreement with the results presented in reference 5. Although on this basis a sharp-nose shape appears slightly better than a blunt-nose shape, reference 5 indicates that the break in the surface contour with a sharp nose causes greater drag than it does with a blunt nose. Unsealing the gap reduced both C_{h_α} and C_{h_δ}, but with the blunt nose (fig. 5(b)) the hinge moments at -15° and -20° deflection became rather irregular. With the gap open, C_{h_α} at zero elevator deflection became positive, which is a desirable characteristic from considerations of free-control stability.

At unstalled angles of attack the elevators having a $0.50c_e$ balance with either a blunt- or a sharp-nose shape (figs. 7 and 8) were overbalanced through some range of deflections. With a sealed gap, the blunt-nose elevator was overbalanced at small deflections (fig. 7(a)); with an open gap, overbalance did not occur until greater than 5° deflection; and, at 15° deflection, the hinge moments became irregular and unsatisfactory (fig. 7(b)). The sharp-nose elevator with the gap both sealed and unsealed was overbalanced at deflections greater than 10° (figs. 8(a) and 8(b)). With the gap sealed, C_{h_α} for both the blunt- and sharp-nose shapes was zero but, with an unsealed gap, the slope became definitely positive.

Because of overbalance, an elevator with a $0.50c_e$ overhang cannot be used without a leading (unbalancing) tab. (See reference 5.) By proper use of such a tab, however, desirable characteristics can be obtained. For example, it is evident from an inspection of figures 8(b) and 18 that a tab deflected -10° when the elevator is deflected -15° will prevent overbalance of the elevator and also increase the lift at this deflection. Thus, if a tab is geared to deflect in the same direction as the elevator throughout the deflection range wherein the elevator is overbalanced, the overbalance can be prevented and the lift effectiveness of the elevator can be increased.

At angles of attack above the stall, such as are encountered in spins, C_{h_δ} for all elevators generally became greater than when the airfoil was unstalled. At angles of attack slightly above the stall, the slope C_{h_α}

was sometimes positive but, at angles of attack far above the stall, it was generally negative and of greater magnitude than at angles of attack below the stall.

The free-floating angle of an elevator at spin attitudes is dependent upon the ratio of C_{h_α} to C_{h_δ} at the angle of attack in question. Thus, because C_{h_δ} is greater for a plain elevator than for a balanced elevator, a plain elevator generally trims at a smaller negative deflection than a balanced elevator. This result indicates that it will require more push force to start moving a balanced elevator off the stop to upset spin equilibrium than it will to start moving a plain elevator. The force required to hold a plain elevator at zero deflection in a spin is, however, greater than that required to hold a balanced elevator of the same chord, although for either elevator the force may be greater than the pilot is capable of exerting.

An examination of figures 4 and 5 indicates that, at the large angles of attack typically encountered in a spin, there was at each angle of attack some negative deflection at which the hinge-moment coefficient was the same for both a plain and a $0.35c_e$ balanced elevator. At more positive deflections the balanced elevator gave smaller hinge moments, but at more negative deflections it gave greater hinge moments than did the plain elevator. It is evident that there can exist a condition where the stick forces of a balanced elevator are greater than those of a plain elevator of the same chord and plan form. This situation is caused by the relative free-floating tendencies of the various elevators at the high angles of attack encountered in a spin. When the dynamic pressure in the spin is such that the stick forces involved approach the maximum a pilot is capable of exerting, it is entirely possible that recovery can be made with a plain elevator when it cannot be made with a balanced elevator. This situation exists only when the deflection required to start recovery is more negative than the deflection at which each elevator has the same hinge-moment coefficient. When it is more positive than this value, exactly the opposite situation can exist; that is, recovery can be made with a balanced but not an unbalanced elevator. The manner in which these generalities apply to any particular airplane can be computed from the data presented if the elevator deflection required to upset the spin equilibrium is known.

The use of a trimming tab presents a convenient and feasible means of reducing the stick forces encountered in a spin to a magnitude the pilot is capable of applying. Figures 14 to 18 indicate a tab to be more effective in changing hinge moments at angles of attack above the stall than below the stall. Thus, at spin attitudes a trimming tab deflected in the same direction as the elevator will shift the free-floating angle of any elevator in such a manner as to reduce the stick forces. An inspection of figure 15(c) indicates that a trimming-tab deflection of about -10° made the $0.35c_e$ blunt-nose elevator float at about the same angle as did the plain elevator at 47.3° angle of attack.

A comparison of blunt-nose and sharp-nose elevators under spin conditions (figs. 4 to 9) indicates that sharp-nose elevators have better free-floating tendencies than blunt-nose elevators; that is, they float at smaller negative deflections. The $0.50c_e$ blunt-nose, balanced elevator with sealed gap (fig. 7(a)) would apparently reach unstable equilibrium at about 20° deflection at spin attitudes.

Parameters

The values of the hinge-moment coefficient parameters presented in figure 19(a) are for blunt-nose elevators and were read from the curves of figures 4, 5, and 7 at 0° angle of attack or elevator deflections. In the interpretations of these parameters it should be remembered that separation phenomena causes nonlinearity of the curves of airfoil characteristics and, therefore, the slopes quoted can apply strictly only over the linear range at which the slope was measured.

The current series of tests indicated (fig. 19(a)) the following trends for blunt-nose balances on the finite tail surface tested. Both C_{h_α} and C_{h_δ} decrease in magnitude as the size of aerodynamic balance is increased. As interpolated from the test data by means of the curves of figure 19, C_{h_α} became zero with about $0.33c_e$ overhang when the gap was unsealed. Likewise, C_{h_δ} became zero with approximately $0.46c_e$ overhang, when the gap was unsealed; but, with open gap, the elevator was not overbalanced at low deflections with a $0.50c_e$ overhang. With overhangs greater than $0.40c_e$, however, the elevator was

probably overbalanced throughout some range of deflection regardless of gap.

Because the lift characteristics were practically unaffected by unsealing the gap and the hinge-moment parameters were reduced, the test results indicate that, for blunt-nose, balanced elevators, a 0.005c gap is more favorable than a sealed gap. For a plain elevator, however, this result is not true because unsealing the gap appreciably reduces the lift. These conclusions are further substantiated by the test results presented in references 2, 3, 4, and 5; a comparison of the measured parameters with the parameters of these references is discussed in a later section of this report.

Effect of Yaw on Elevator Hinge Moments

Because the current series of tests were made without a wing on the model, the characteristics of the horizontal tail cannot, of course, be affected by movement of the tail away from the region of strong downwash at the center of the wing as the complete airplane is yawed. Being independent of this effect, the characteristics presented as a function of angle of yaw may be considered as applying to an airplane whose horizontal tail lies entirely clear of the wing downwash or as being a component part of the total effect for a complete airplane. This fact should be borne in mind when interpreting the data of figures 9 to 13.

As indicated in figures 9 to 13, angles of yaw up to 20° throughout the unstalled-flight range and angles of yaw up to 10° throughout the stalled-flight range affected only slightly the hinge-moment coefficients of all elevators tested. As the model was yawed beyond 20°, the increment of hinge-moment coefficient caused by angle of yaw generally was negative and increased rapidly in magnitude up to some critical value of angle of yaw inversely dependent on the angle of attack. As the model was yawed still farther, the negative increments of hinge-moment coefficient decreased in magnitude and sometimes at the highest angles of yaw tested the increment became positive. Figures 9 to 13 clearly indicate the variation of increment of elevator hinge-moment coefficient as a function of angle of yaw for each elevator tested. At large unstalled angles of attack, the negative increments of hinge moment caused by angle of yaw tend to compensate for the increased

stick force due to the larger negative elevator deflections required in order to maintain constant speed as the airplane is sideslipped when landing.

Effect of Tab on Elevator Hinge Moments

With the elevator neutral, the tab was most effective in changing the elevator hinge-moment coefficient at 0° angle of attack and became less effective as the angle of attack increased either positively or negatively in the unstalled range. At angles of attack beyond the stall, the tab often gave increments of hinge-moment coefficient approaching in magnitude the values below the stall. Parts (a) of figures 14 to 18 present this variation for all elevators tested. Figure 17(a) indicates that, for a $0.50c_e$ blunt-nose elevator, the hinge-moment effectiveness of the tab was greater beyond the stall than below the stall but, below the stall, the increments were much smaller for this elevator than for the other elevators tested. Because of the large amount of overhang on the $0.50c_e$ balanced elevator this result might be expected.

The variation of increment of elevator hinge-moment coefficient caused by $\pm 10^\circ$ tab deflection as a function of elevator deflection (parts (b) and (c) of figs. 14 to 18) was not consistent for the various elevators tested. There existed a tendency, however, for the increment to be fairly constant for elevator deflections less than 10° for all elevators except the plain and the $0.50c_e$ balanced blunt-nose elevator, which were quite erratic. At deflections greater than 10°, the increments generally became smaller.

Because the tab maintains its effectiveness in changing the elevator hinge moments at angles of attack beyond the stall, it can, as has been previously pointed out, be used as a trimming device in a spin. By an upward (negative) deflection of the tab the free-floating angle of an elevator can be reduced in a spin and, consequently, the stick forces can be lowered. Thus, by proper use of a trimming tab it should be possible to recover from a spin when, without the use of the tab, recovery might be impossible.

Drag

Because of the small size of the tail surface tested, the relative drag characteristics of the various elevators could not be measured with sufficient precision to make the results conclusive. The differences in drag coefficient of the various surfaces was less than the limits of experimental accuracy previously discussed. Based on the tail area, the minimum drag coefficient of the fuselage-tail combination, however, was determined to be 0.0580 for all elevators.

Profile-drag coefficients are presented in references 2, 3, and 5 for elevators similar to the ones tested in the present investigation. These two-dimensional-flow data indicated that the profile-drag coefficient of a blunt-nose elevator at 0° deflection and 0° angle of attack was the same for all sizes of aerodynamic balance. Because of the abrupt break in the control surface, a sharp-nose balance gave an increment in minimum profile-drag coefficient of 0.0024 for the $0.35c_e$ overhang and 0.0042 for the $0.50c_e$ overhang. (See references 2, 3, and 5.)

Comparison with Two-Dimensional Data

Characteristics of the plain elevator were computed from the two-dimensional-flow data of reference 1 modified to agree with later force-test measurements (reference 2), which are believed to be a bit more accurate. The lift correction for aspect ratio was made in accordance with the method presented in reference 8, and the hinge moments were corrected in the manner discussed in reference 1. The following table compares the computed and measured values of certain parameters for the plain sealed elevator:

L-379

Parameter	Computed value	Measured value
$\left(\frac{\partial C_L}{\partial \alpha}\right)_\delta$	0.057	0.053
$\left(\frac{\partial \alpha}{\partial \delta}\right)_{C_L}$	-.54	-.53
$\left(\frac{\partial C_h}{\partial \alpha}\right)_\delta$	-.0035	-.0009
$\left(\frac{\partial C_h}{\partial \delta}\right)_\alpha$	-.0100	-.0086

It is to be expected that fuselage interference will affect the characteristics of the horizontal tail. The manner of computing this effect, however, is as yet unknown and, therefore, the computed parameters apply to the isolated tail surface rather than to the fuselage-tail combination tested. If it is assumed that the fuselage interference caused the discrepancy between the computed and the measured value of the slope of the lift curve then, when the measured C_{L_α} is arbitrarily used for computations of the hinge-moment coefficient parameters, C_{h_α} becomes -0.0033 and C_{h_δ} becomes -0.0099.

The calculated lift effectiveness $\left(\frac{\partial \alpha}{\partial \delta}\right)_{C_L}$ agrees well with the measured value, but it is apparent that a fuselage-interference factor must be applied to correct the calculated slope of the lift curve, which is slightly greater than the measured value. The hinge-moment parameters, however, in addition to requiring an interference factor are probably considerably affected by plan form in a manner as yet unknown. Because of these unknown factors, finite-tail-surface characteristics computed from two-dimensional-flow data by the method described in reference 1 give no better agreement with measured values than computations based on an average flap-chord ratio for the entire surface.

The values of the hinge-moment parameters as a function of aerodynamic balance for a finite-aspect-ratio and an infinite-aspect-ratio airfoil are given in figure 19. The plain unbalanced elevator, because it is hinged at the center of the nose radius, does have about a 9-percent elevator-chord overhang. This overhang, however, can contribute no balancing effect because all forces normal to the surface of the overhang act through the hinge axis.

The absolute magnitude of the parameters in two- and three-dimensional flow, of course, should not be expected to agree. The general trend of variation of the parameters with balance and the effect of gap, however, is similar. The point at which the curves of figure 19 cross zero is largely dependent upon the measured value of the parameters for a $0.50c_e$ balanced elevator. An inspection of figure 7 shows that the sign and the magnitude of C_{h_δ} depends largely upon what deflection range is under consideration. Hence, all that can be said with certainty is that, in both two- and three-dimensional flow a $0.35c_e$ overhang did not produce overbalance but a $0.50c_e$ overhang did throughout some range of deflection. With some intermediate overhang, both section data and finite-airfoil data indicated that the elevator became overbalanced. In three-dimensional flow, C_{h_α} became zero with a smaller amount of balance than would be predicted from section data.

CONCLUSIONS

The following general conclusions, based on the measured aerodynamic characteristics of the various tail surfaces tested in the current investigation, were drawn:

1. The lift effectiveness of the elevator was practically independent of the size and the shape of the aerodynamic balance. The effective deflection range was, however, decreased for the balanced elevators.

2. At angles of attack below the airfoil stall the maximum deflection to which an elevator was effective in producing an increment of lift when deflected in opposition to the angle of attack was approximately equal to the unporting angle of the elevator balance and was somewhat affected by the elevator nose shape and the gap.

3. If, at angles of attack far above the stall, the elevator can be moved, increments of lift can be obtained to effect a recovery from a spin.

4. The effect of aerodynamic balance was to reduce the elevator hinge moments so that, for a blunt nose shape, the slope of elevator hinge-moment coefficient curve with respect to angle of attack became zero with about 33 percent elevator chord balance when the gap was open and with about 50-percent elevator chord when the gap was sealed. Regardless of gap or nose shape, the elevator with a 35-percent elevator-chord overhang was not overbalanced but, with a 0.50 elevator-chord overhang, it was always overbalanced throughout some range of deflections.

5. It appears possible that recovery from a spin can be effected with a plain elevator and not with a balanced elevator or, conversely, with a balanced elevator and not with a plain elevator, depending upon the dynamic pressure and the elevator deflection required to upset the spin equilibrium.

6. Under spin conditions, a trim tab deflected in the same direction as the elevator presents a convenient and feasible means of reducing the stick forces of an elevator to a magnitude the pilot should be capable of handling.

7. The effect of angle of yaw on the characteristics of the isolated fuselage-tail combination was generally such as to oppose the effects on a complete airplane caused by motion of the tail away from the region of strong downwash as the airplane is yawed.

8. Although fairly close agreement was found between the measured lift characteristics and those computed from two-dimensional-flow data, an interference factor for both lift and hinge moments is required. A plan form factor for hinge-moment characteristics is also necessary before they can be satisfactorily computed from section data.

9. The data indicate that, with a control surface having a large overhang and an unbalancing tab, the control forces can be reduced to any desiredmagnitude, the stick-free stability can be made equal to or greater than the stick-fixed stability, and the control effectiveness can be made equal to or greater than that of a plain flap of the same chord.

Langley Memorial Aeronautical Laboratory,
National Advisory Committee for Aeronautics,
Langley Field, Va.

REFERENCES

1. Ames, Milton B., Jr., and Sears, Richard I.: Determination of Control-Surface Characteristics from NACA Plain-Flap and Tab Data. T.N. No. 796, NACA, 1941.

2. Sears, Richard I.: Wind-Tunnel Investigation of Control-Surface Characteristics. I - Effect of Gap on the Aerodynamic Characteristics of an NACA 0009 Airfoil with a 30-Percent-Chord Plain Flap. NACA A.R.R., June 1941.

3. Sears, Richard I., and Hoggard, H. Page, Jr.: Wind-Tunnel Investigation of Control-Surface Characteristics. II - A Large Aerodynamic Balance of Various Nose Shapes with a 30-Percent-Chord Flap on an NACA 0009 Airfoil. NACA A.R.R., August 1941.

4. Ames, Milton B., Jr.: Wind-Tunnel Investigation of Control-Surface Characteristics. III - A Small Aerodynamic Balance of Various Nose Shapes Used with a 30-Percent-Chord Flap on an NACA 0009 Airfoil. NACA A.R.R., August 1941.

5. Ames, Milton B., Jr., and Eastman, Donald R., Jr.: Wind-Tunnel Investigation of Control-Surface Characteristics. IV - A Medium Aerodynamic Balance of Various Nose Shapes Used with a 30-Percent-Chord Flap on an NACA 0009 Airfoil. NACA A.R.R., Sept. 1941.

6. Harris, Thomas A.: The 7 by 10 Foot Wind Tunnel of the National Advisory Committee for Aeronautics. Rep. No. 412, NACA, 1931.

7. Wenzinger, Carl J., and Harris, Thomas A.: Wind-Tunnel Investigation of an N.A.C.A. 23012 Airfoil with Various Arrangements of Slotted Flaps. Rep. No. 664, NACA, 1939.

8. Jones, Robert T.: Correction of the Lifting-Line Theory for the Effect of Chord. T.N. No. 817, NACA, 1941.

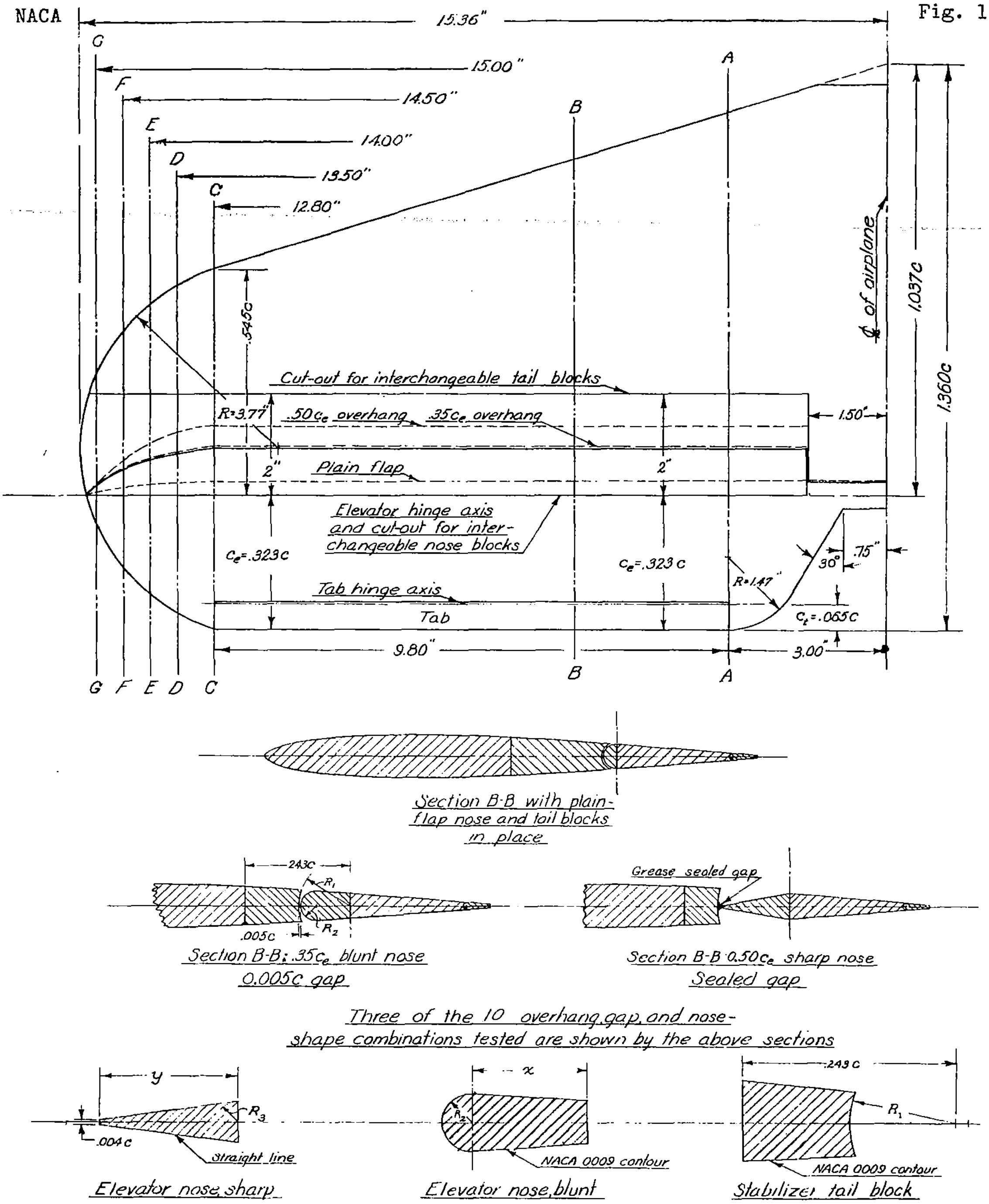

Section	Stabilizer tail block, Balance, percent 0	35	50	Elevator nose, blunt, Balance, percent 0		35		50		Elevator nose, sharp, Balance, percent 0		35		50	
	R_1	R_1	R_1	x	R_2	x	R_2	x	R_2	y	R_3	y	R_3	y	R_3
A-A	0.095	0.118	0.166	0	0.030	0.077	0.036	0.123	0.039	NONE		0.113	0.030	0.161	0.030
C-C	.053	.118	.166	0	.028	.080	.033	.126	.035	NONE		.113	.028	.161	.028
D-D	.090	.104	.147	0	.025	.070	.029	.111	.031	NONE		.099	.025	.142	.025
E-E	.026	.089	.125	0	.021	.060	.024	.093	.027	NONE		.084	.021	.120	.021
F-F	.021	.067	.094	0	.016	.043	.019	.068	.021	NONE		.062	.016	.089	.016
G-G	.012	.034	.046	0	.007	.020	.009	.031	.010	NONE		.029	.007	.041	.007

Dimensions in terms of mean geometric chord, c (8.245 in.)

Figure 1.- Details of horizontal tail.

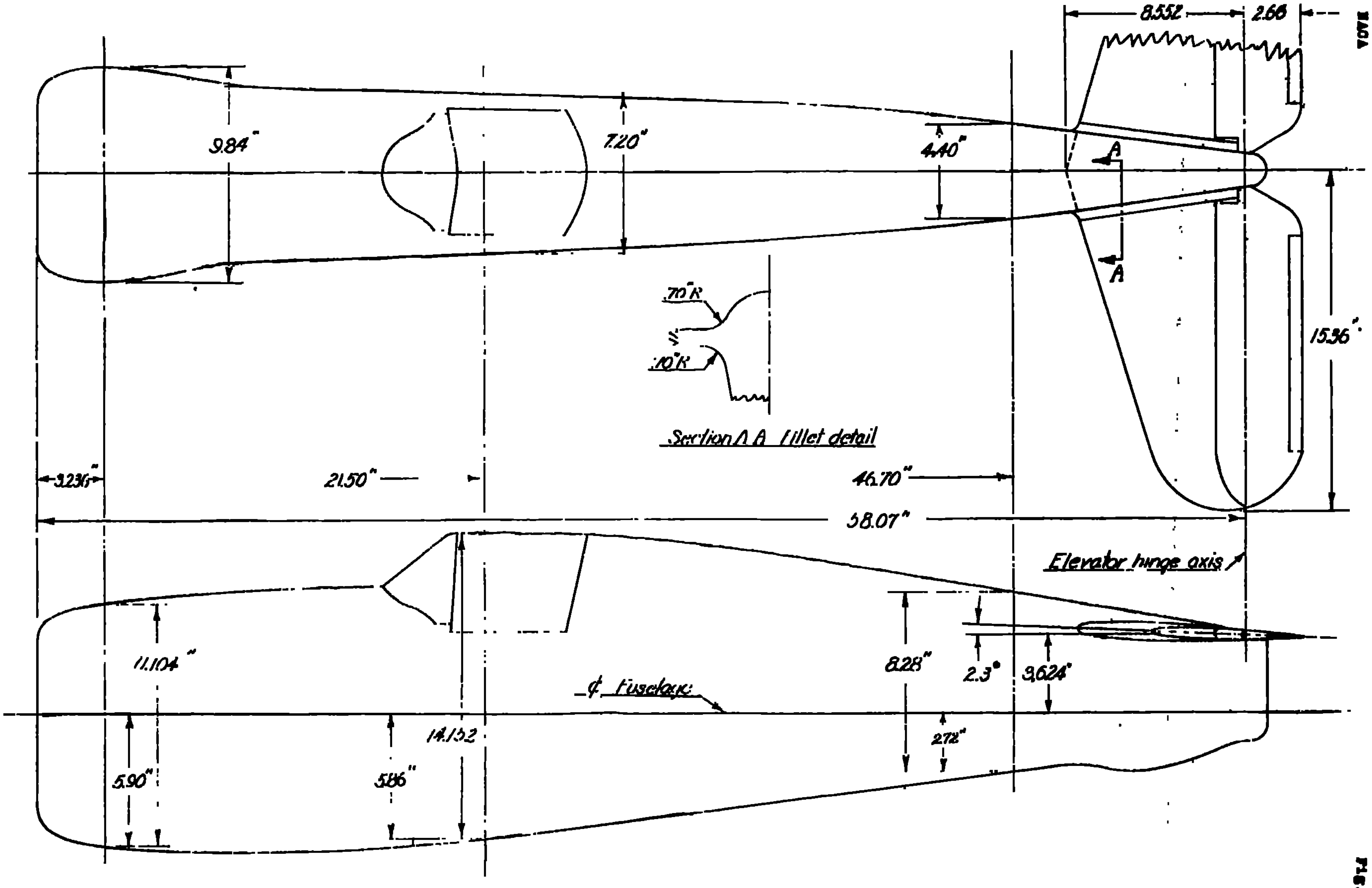

Figure 2.- Horizontal tail mounted on a typical pursuit fuselage.

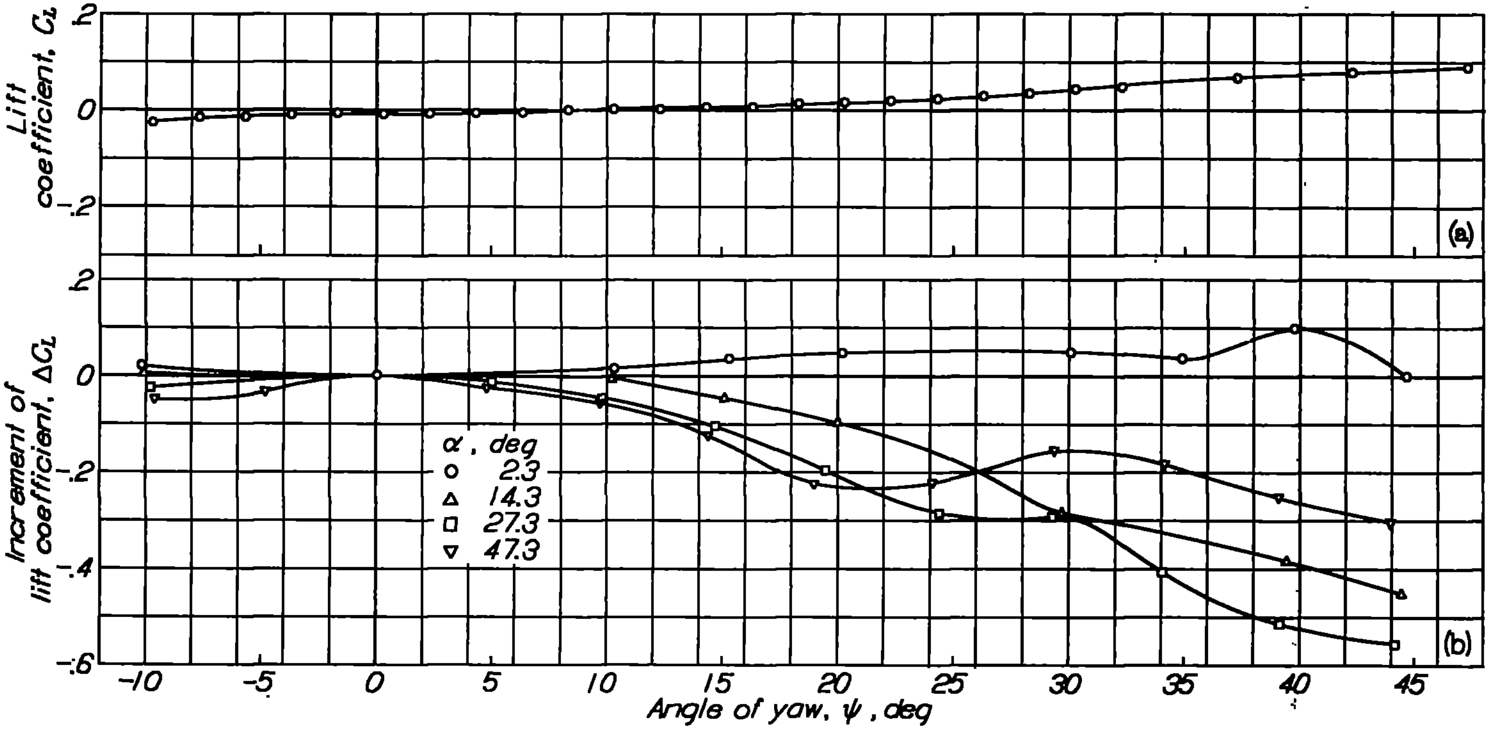

(a) $\psi = 0°$

(b) Four values of α

Figure 3(a,b).- Lift characteristics of fuselage alone as a function of both angle of attack and angle of yaw.

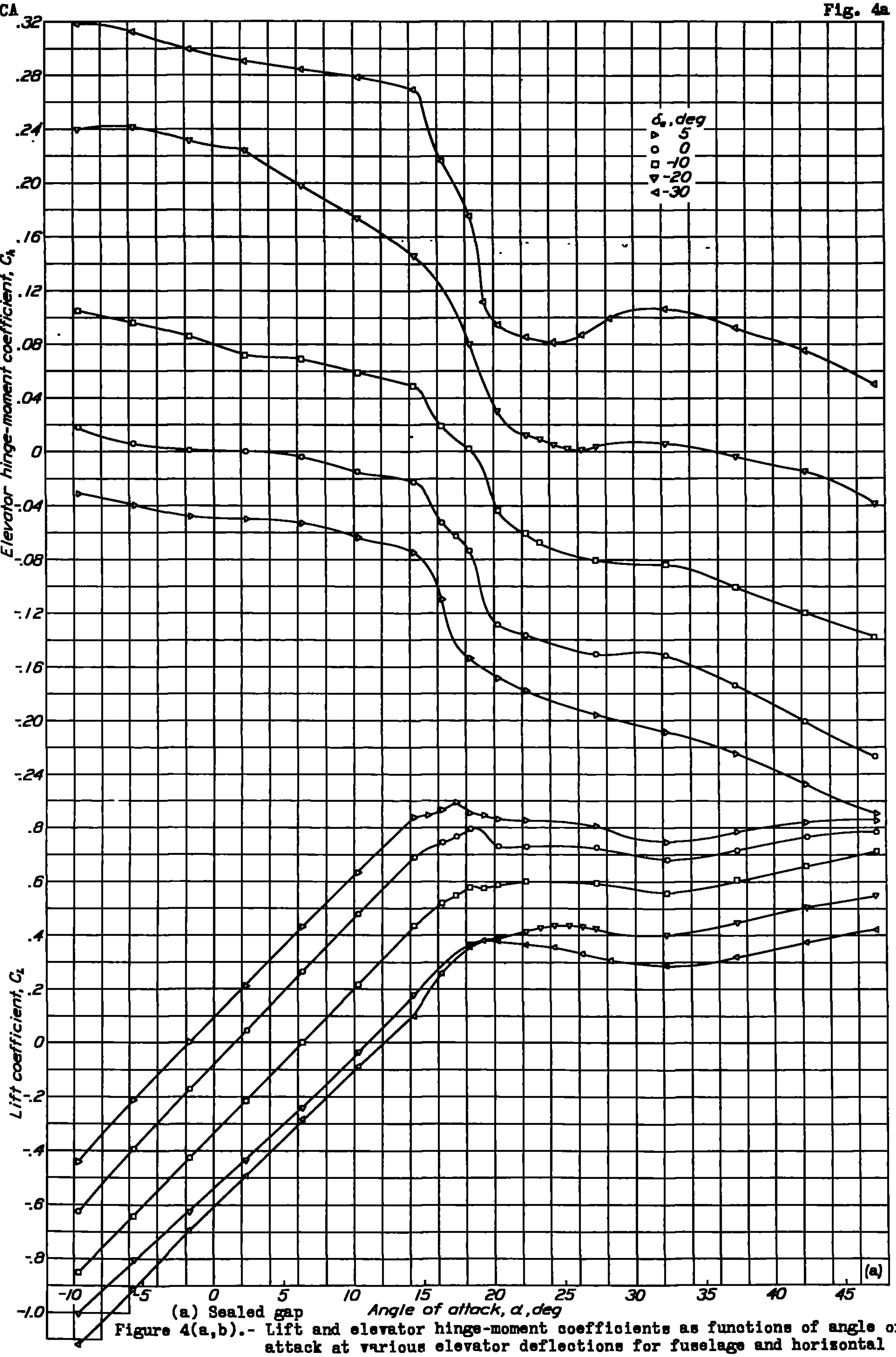

(a) Sealed gap

Figure 4(a,b).- Lift and elevator hinge-moment coefficients as functions of angle of attack at various elevator deflections for fuselage and horizontal tail combination. Plain elevator.

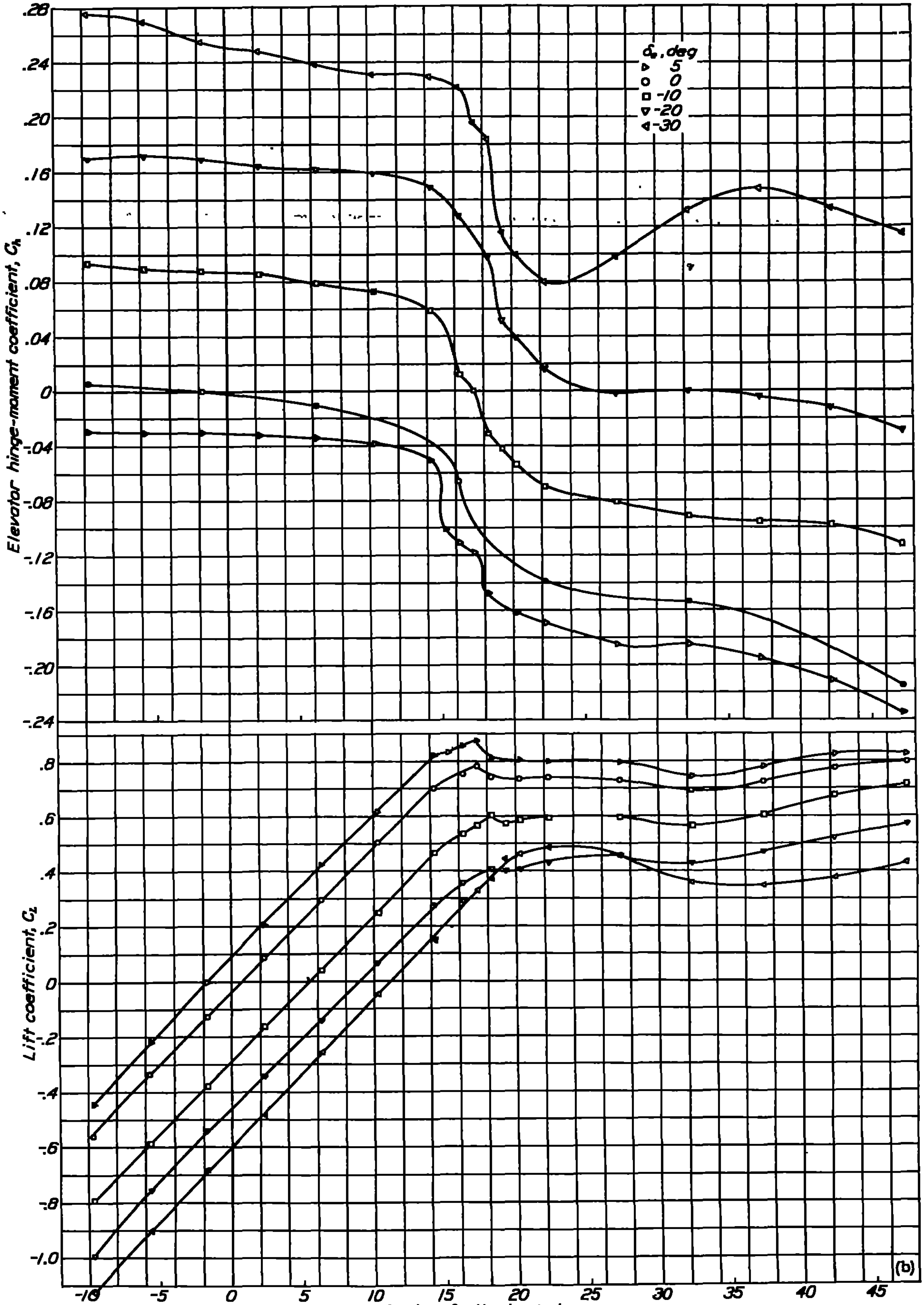

(b) 0.005c gap

Figure 4.- (Concluded)

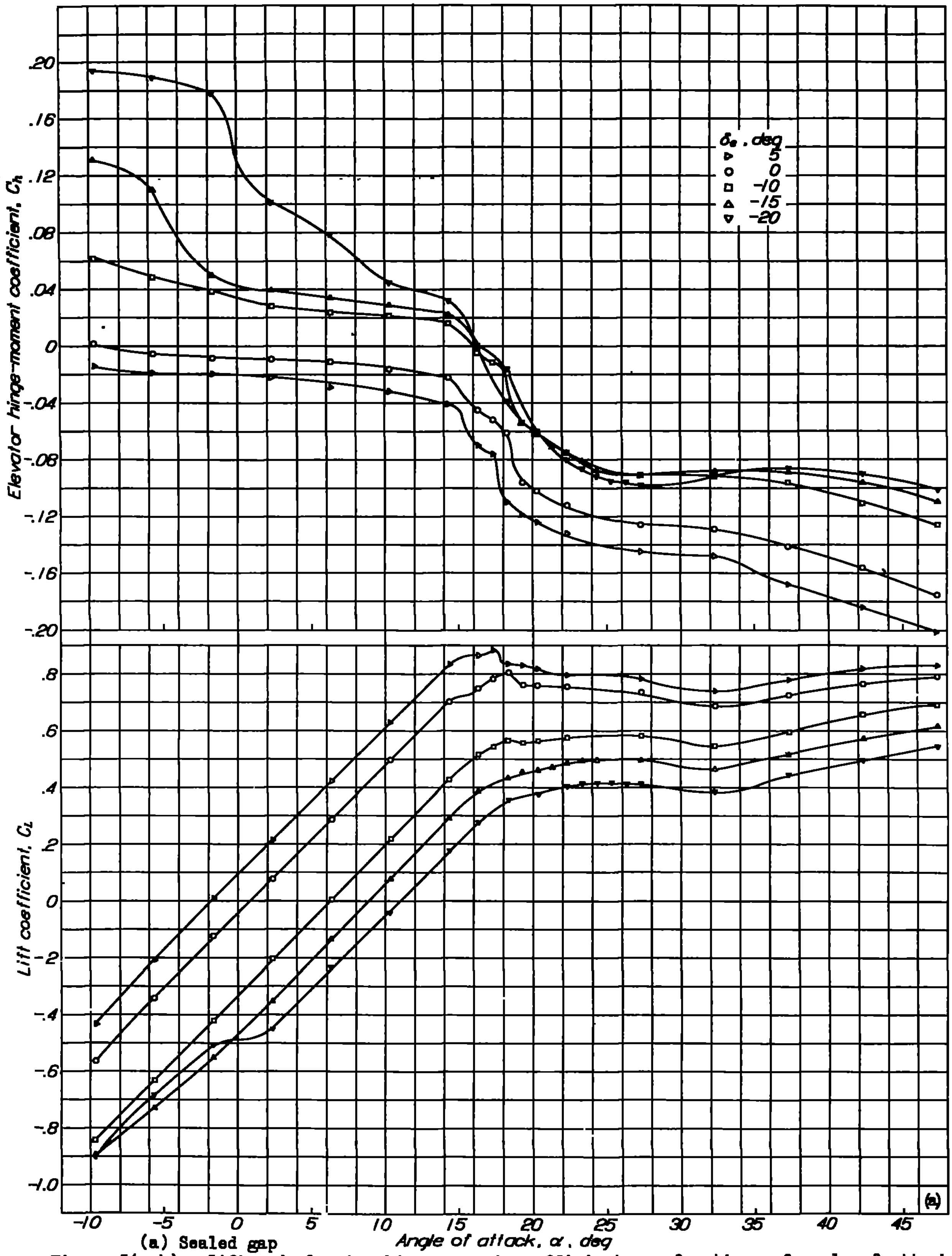

(a) Sealed gap

Figure 5(a,b).- Lift and elevator hinge-moment coefficients as functions of angle of attack at various elevator deflections for fuselage and horizontal tail combination. Balanced elevator with $0.35c_e$ blunt nose overhang.

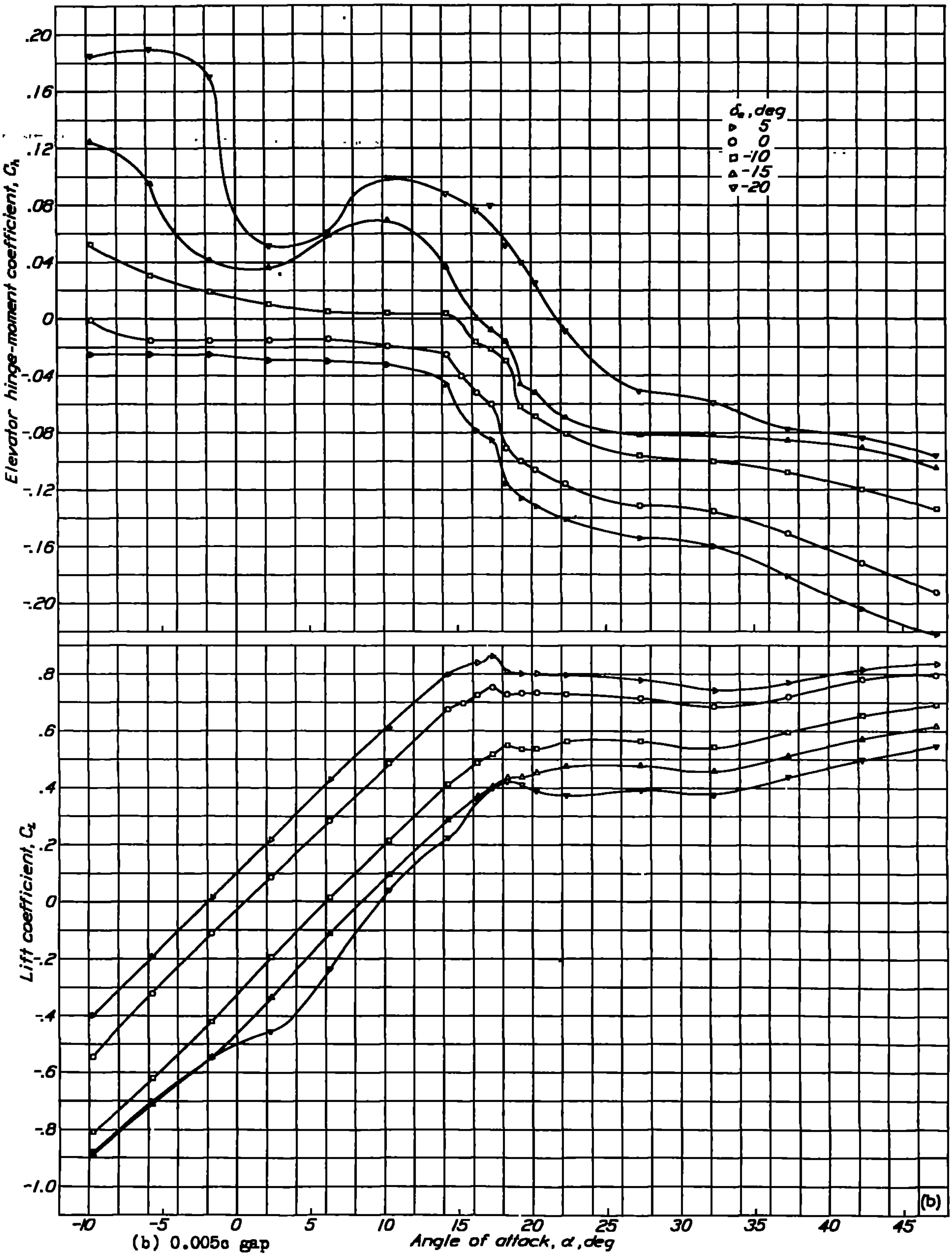

(b) 0.005c gap

Figure 5.- (Concluded)

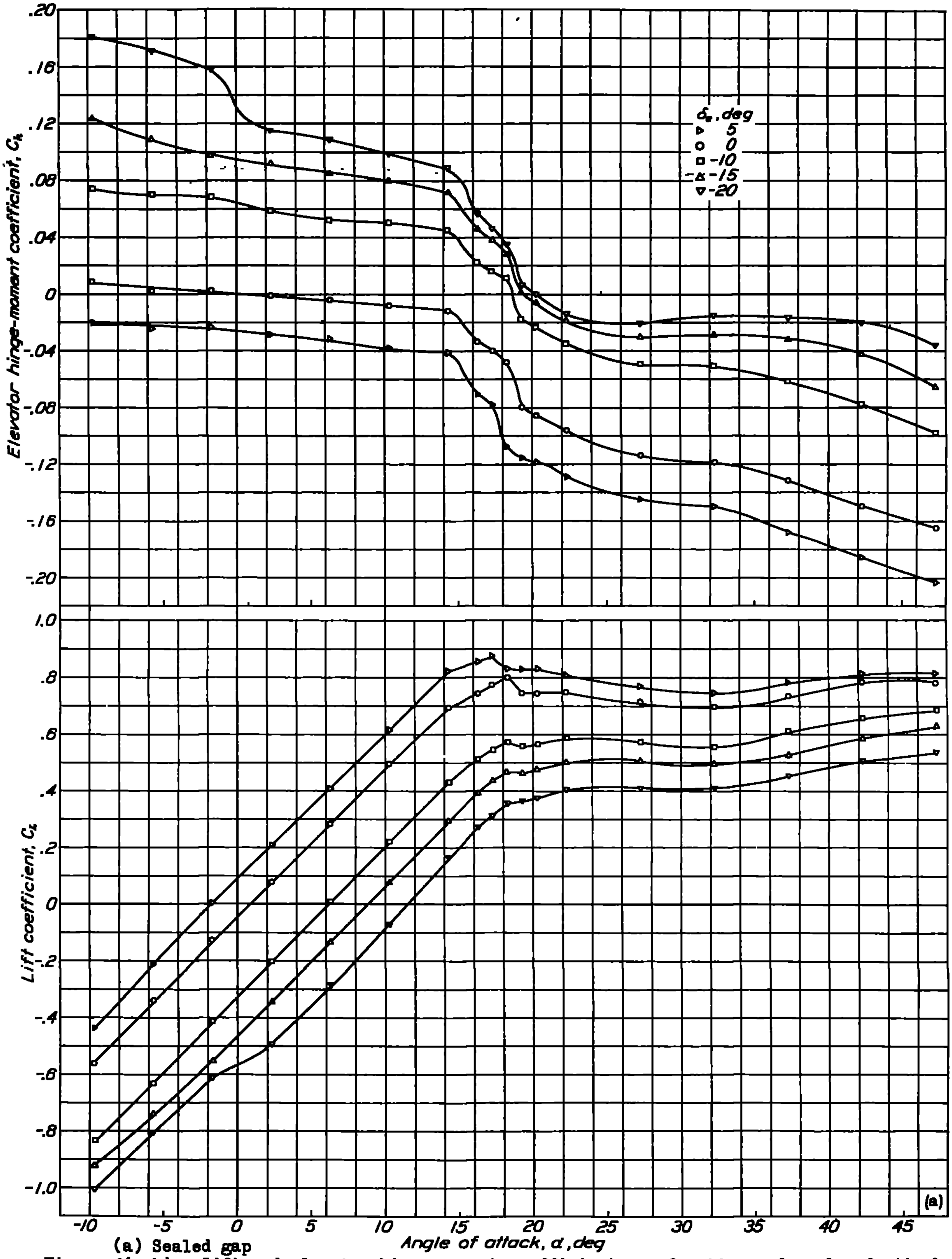

(a) Sealed gap

Figure 6(a,b).- Lift and elevator hinge-moment coefficients as functions of angle of attack at various elevator deflections for fuselage and horizontal tail combination. Balanced elevator with $0.35c_e$ sharp nose overhang.

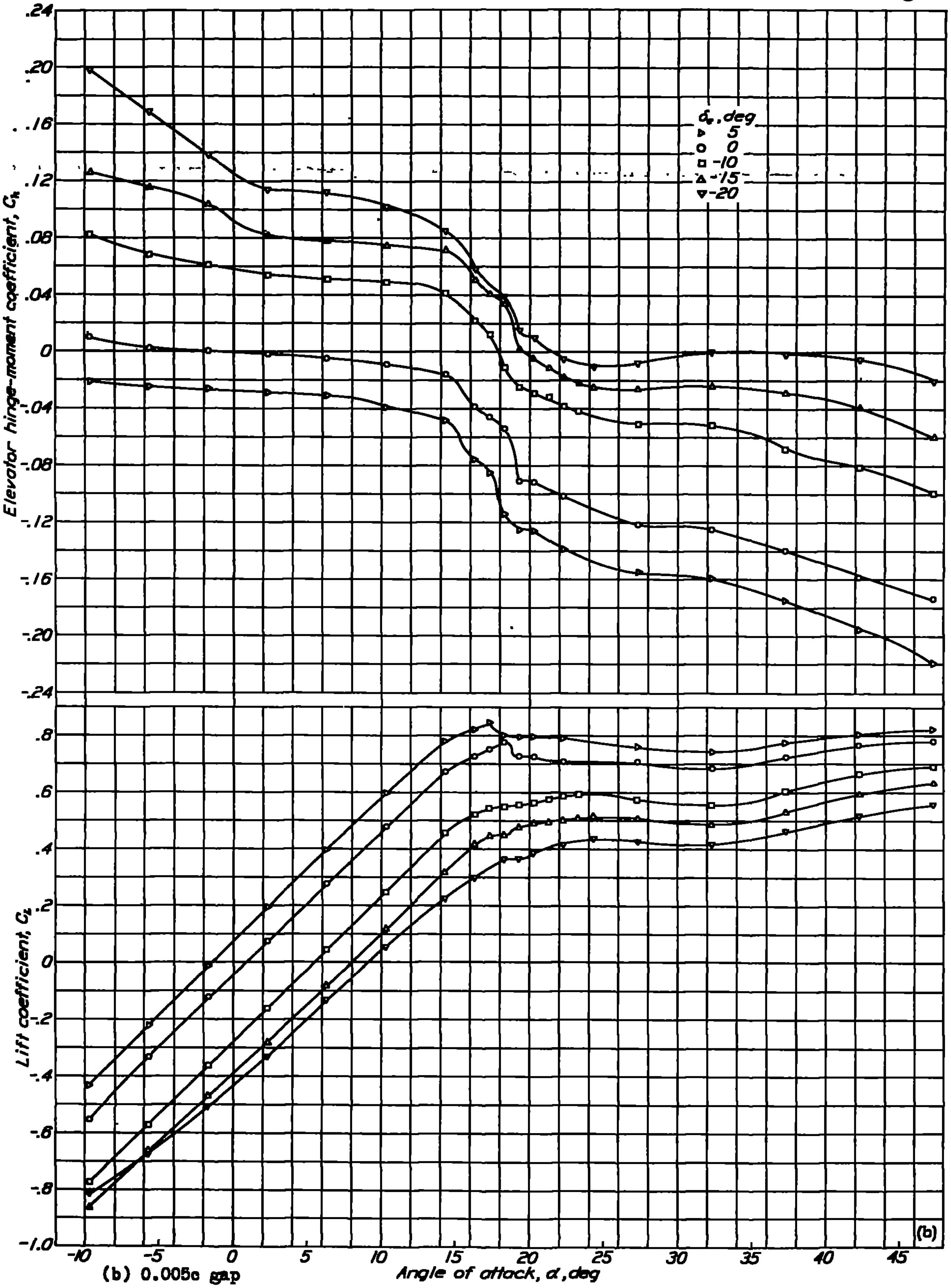

(b) 0.005c gap

Figure 6.- (Concluded)

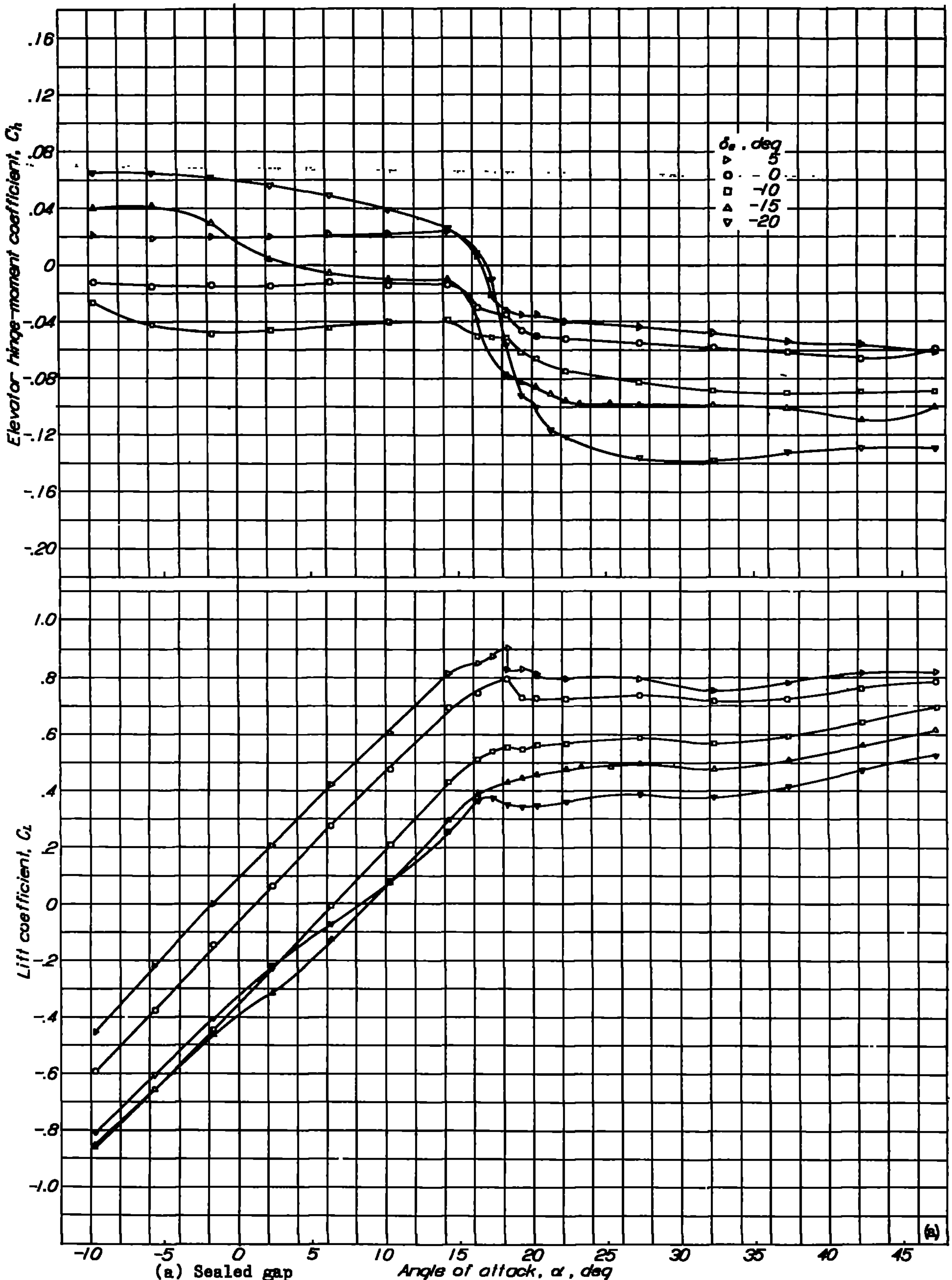

(a) Sealed gap

Figure 7(a,b).- Lift and elevator hinge-moment coefficients as functions of angle of attack at various elevator deflections for fuselage and horizontal tail combination. Balanced elevator with $0.50c_e$ blunt nose overhang.

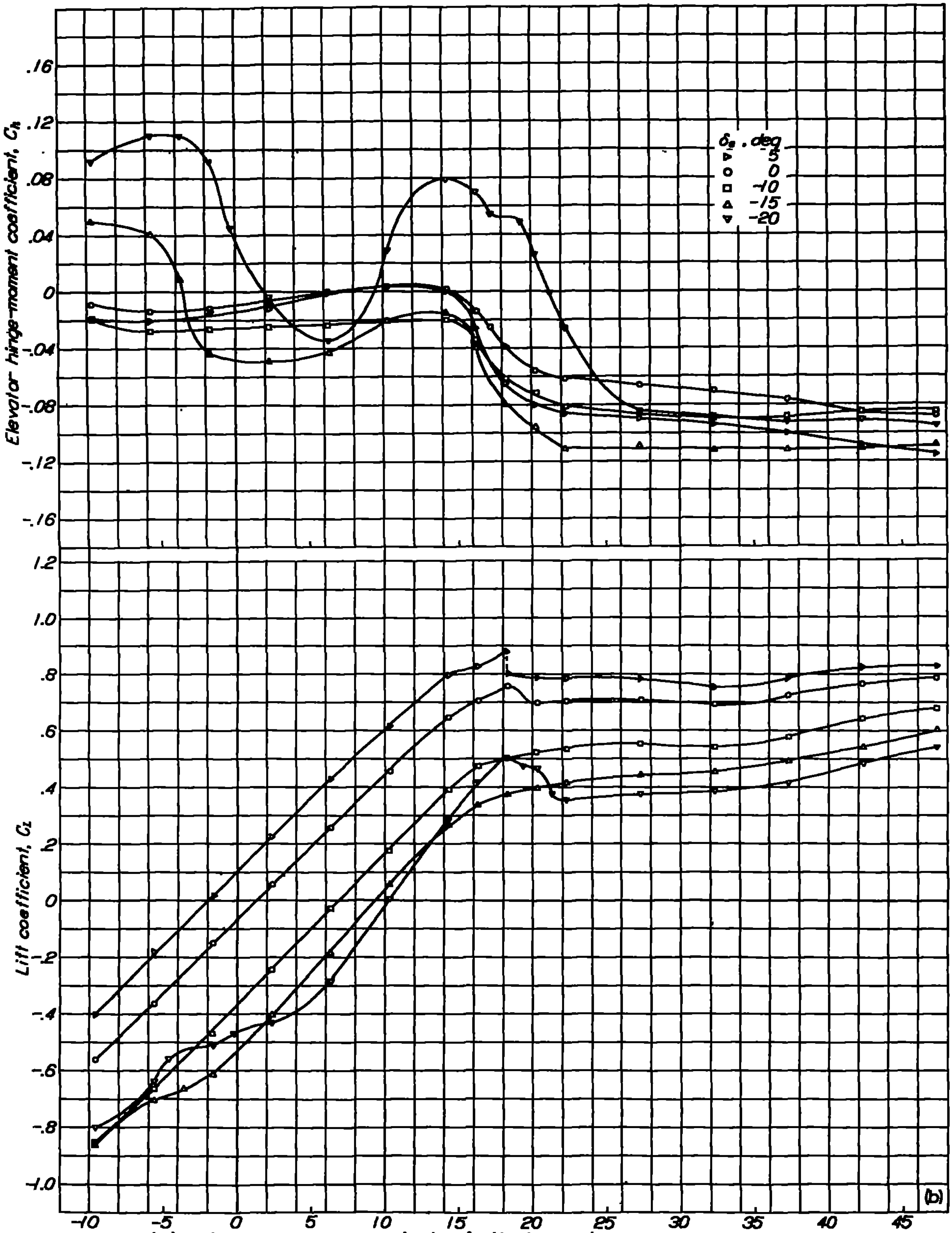

(b) 0.005c gap

Figure 7.- (Concluded)

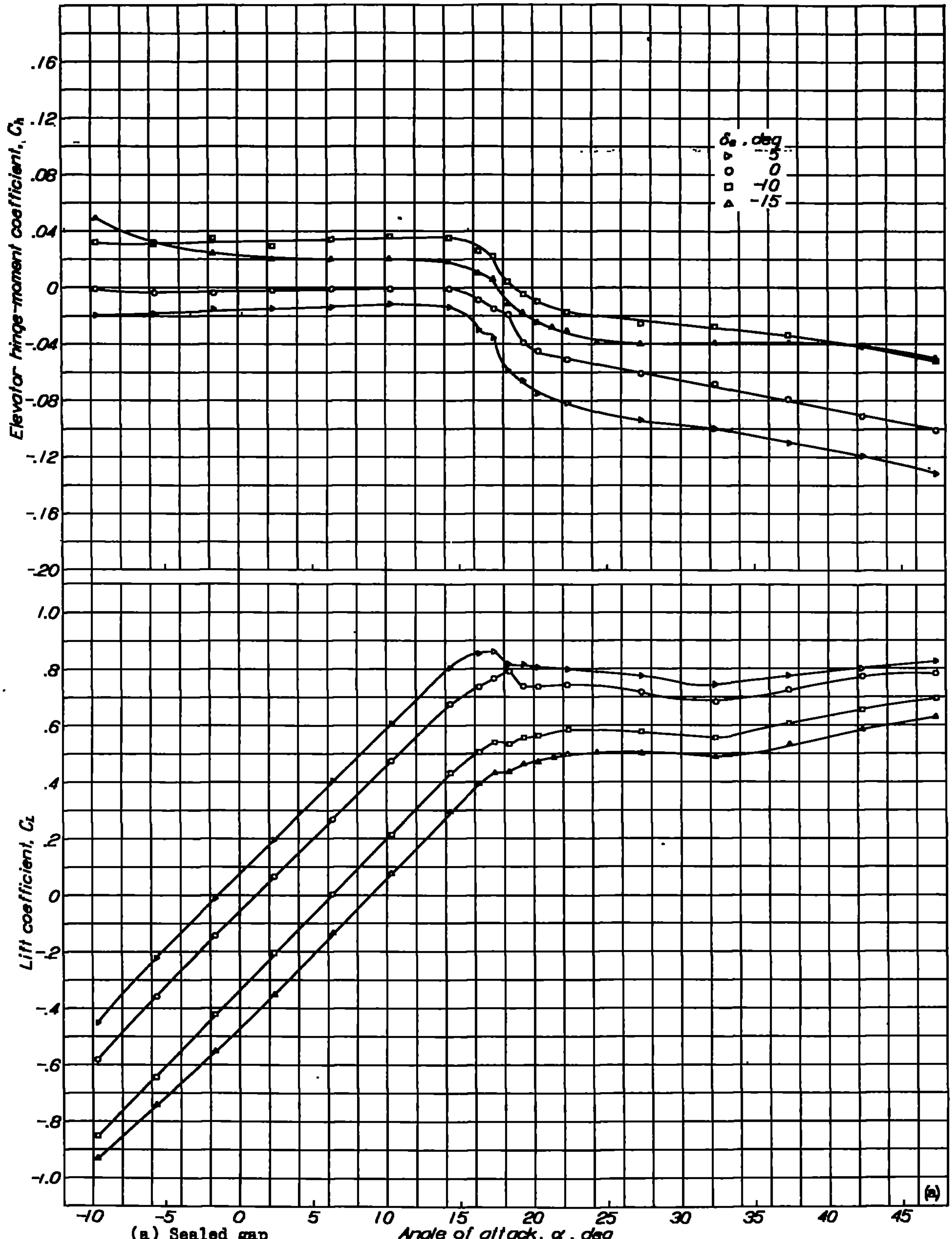

(a) Sealed gap

Figure 8(a,b).- Lift and elevator hinge-moment coefficient as functions of angle of attack at various elevator deflections for fuselage and horizontal tail combination. Balanced elevator with $0.50c_e$ sharp nose overhang.

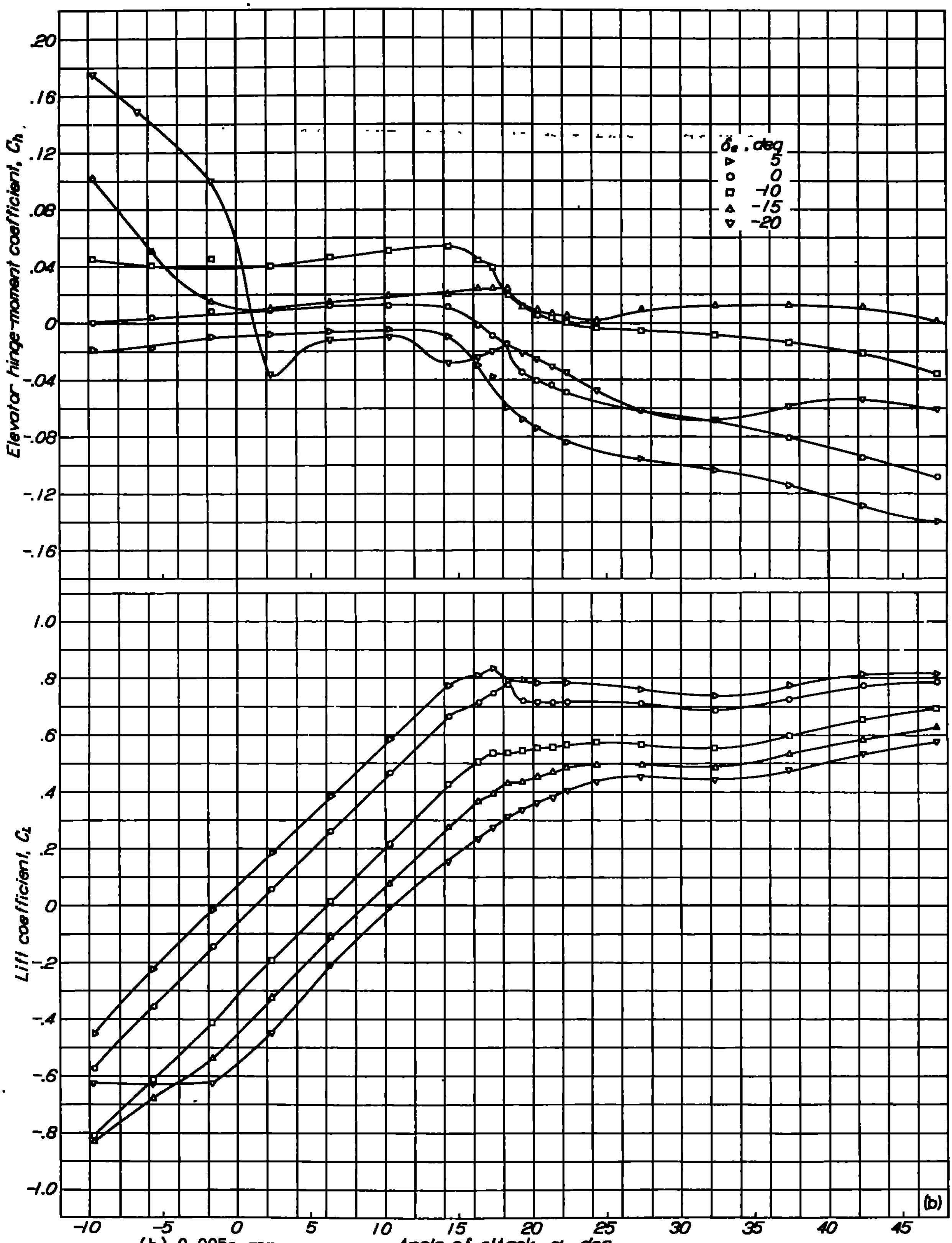

(b) 0.005c gap

Figure 8.- (Concluded)

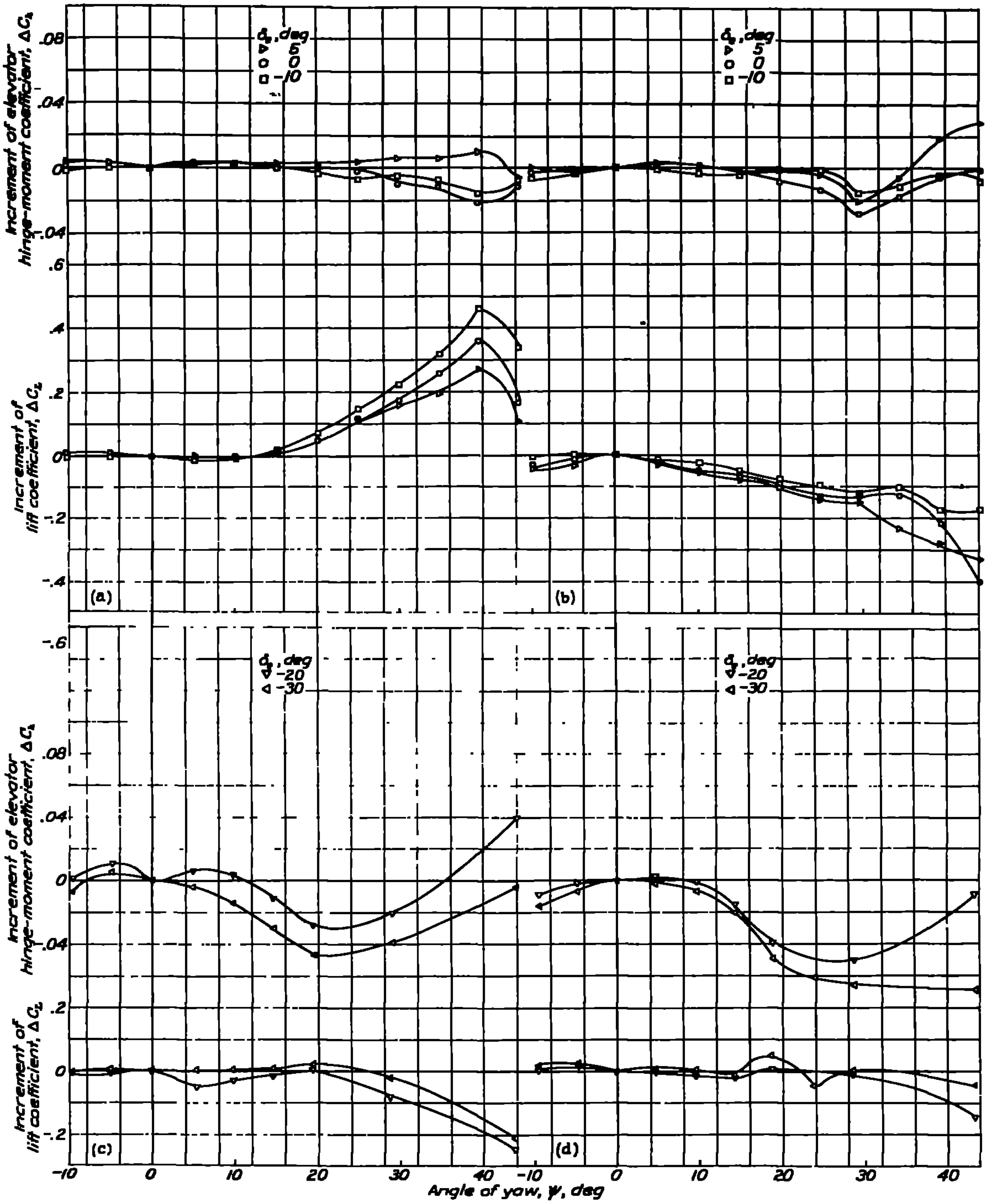

(a) $\alpha = 2.3^{\circ}$ (b) $\alpha = 14.3^{\circ}$ (c) $\alpha = 27.3^{\circ}$ (d) $\alpha = 47.3^{\circ}$

Figure 9.- Increments of lift and elevator hinge-moment coefficients due to angle of yaw as functions of angle of yaw at various angles of attack and elevator deflections. Plain elevator with sealed gap.

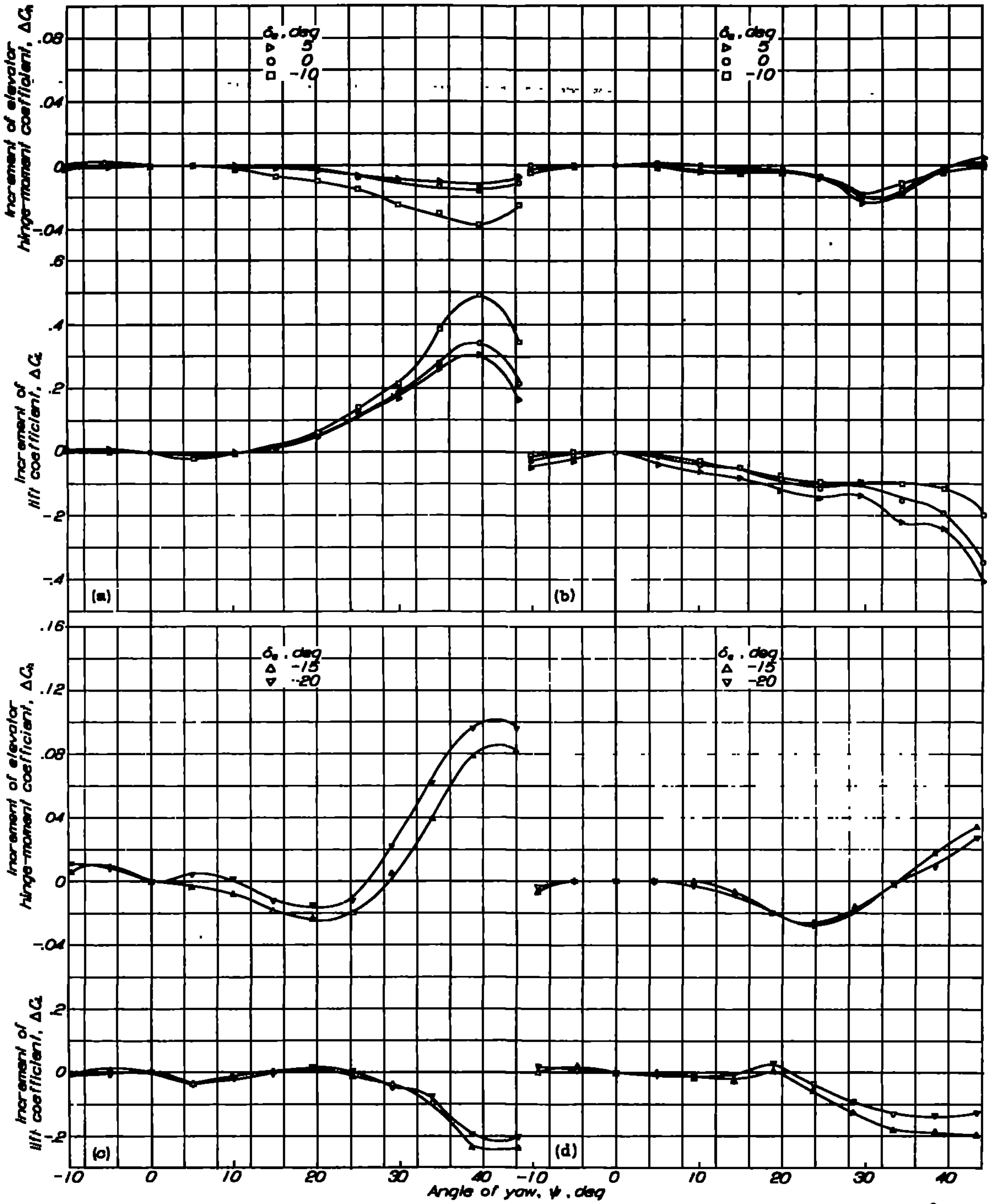

(a) α = 2.3° (b) α = 14.3° (c) α = 27.3° (d) α = 47.3°

Figure 10.- Increments of lift and elevator hinge-moment coefficients due to angle of yaw as functions of angle of yaw at various angles of attack and elevator deflections. Balanced elevator with $0.35c_e$ blunt nose overhang and sealed gap.

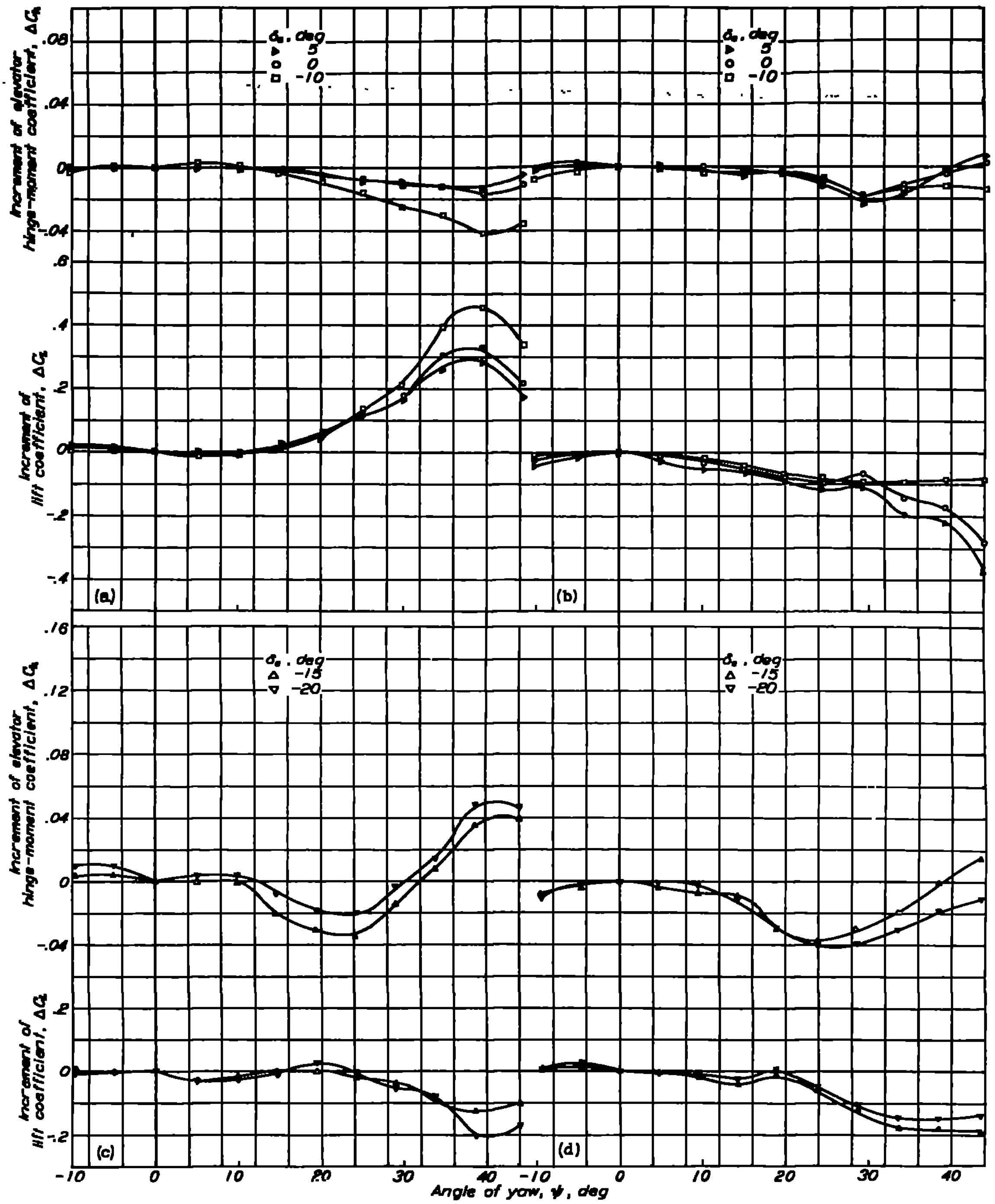

(a) $\alpha = 2.3^\circ$ (b) $\alpha = 14.3^\circ$ (c) $\alpha = 27.3^\circ$ (d) $\alpha = 47.3^\circ$

Figure 11.- Increments of lift and elevator hinge-moment coefficients due to angle of yaw as functions of angle of yaw at various angles of attack and elevator deflections. Balanced elevator with $0.35c_e$ sharp nose overhang and sealed gap.

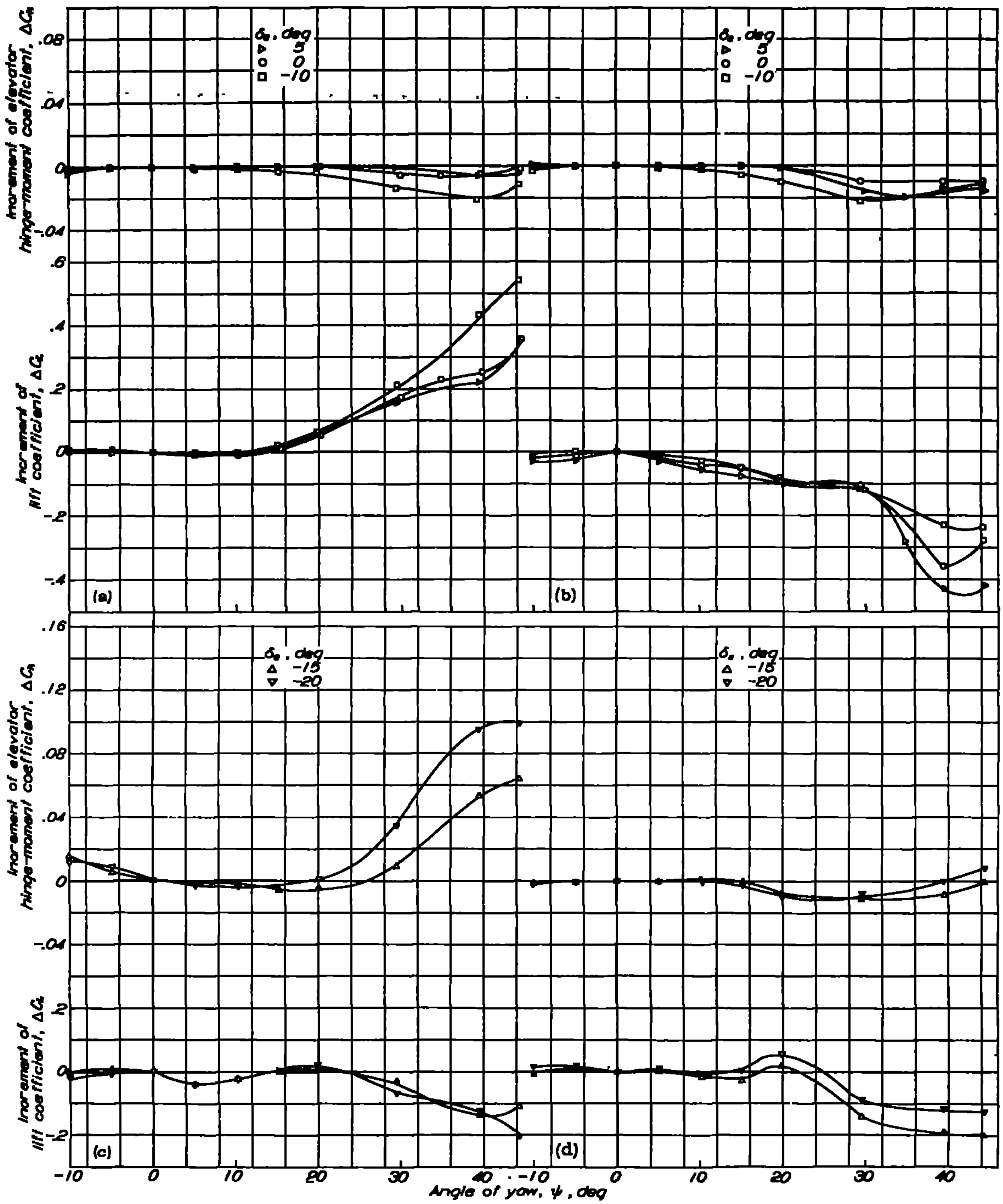

(a) α = 2.3° (b) α = 14.3° (c) α = 27.3° (d) α = 47.3°

Figure 12.- Increments of lift and elevator hinge-moment coefficients due to angle of yaw as functions of angle of yaw at various angles of attack and elevator deflections. Balanced elevator with $0.50c_e$ blunt nose overhang and sealed gap.

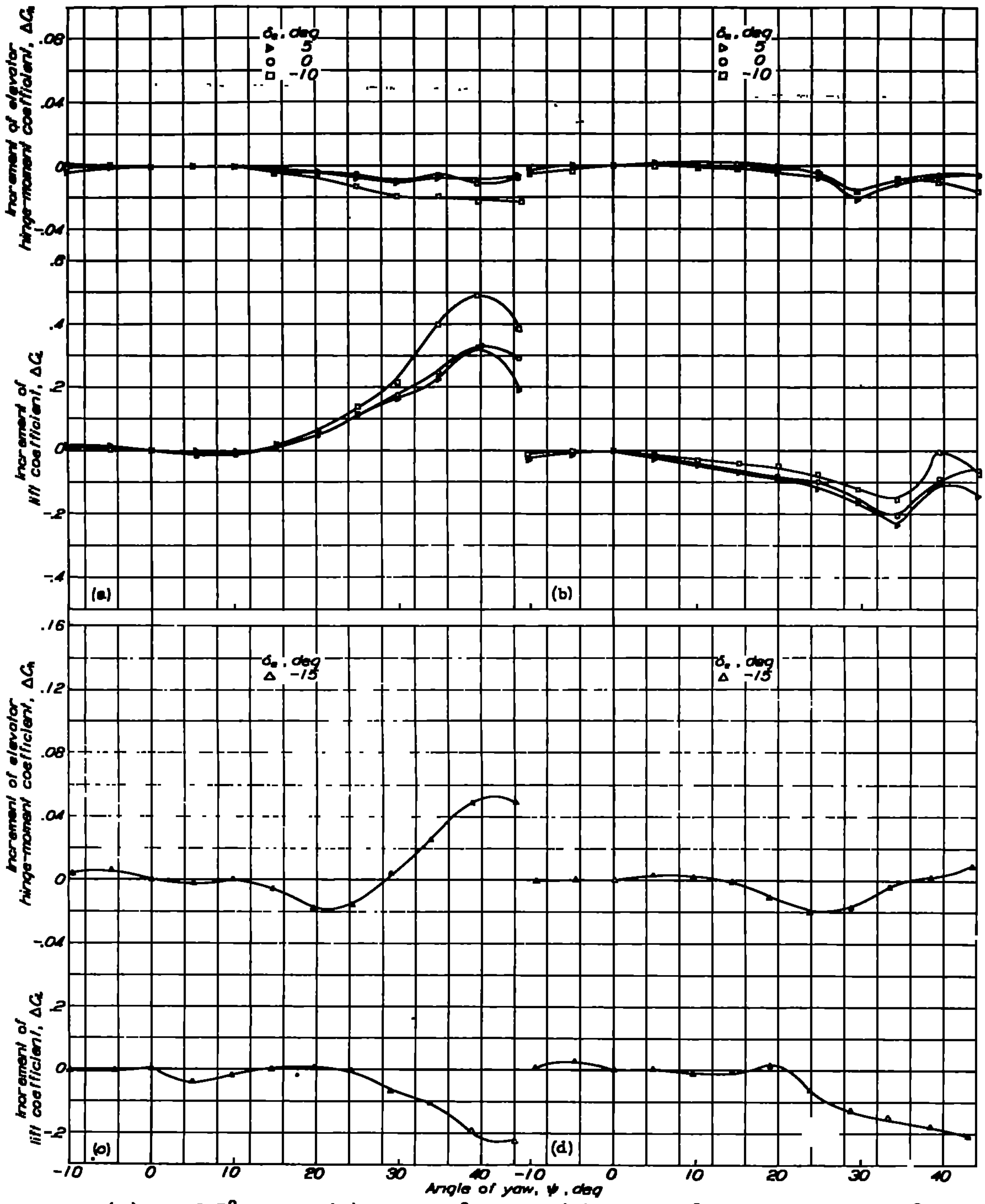

(a) $\alpha = 2.3^{\circ}$ (b) $\alpha = 14.3^{\circ}$ (c) $\alpha = 27.3^{\circ}$ (d) $\alpha = 47.3^{\circ}$

Figure 13.- Increments of lift and elevator hinge-moment coefficients due to angle of yaw as functions of angle of yaw at various angles of attack and elevator deflections. Balanced elevator with $0.50c_e$ sharp nose overhang and sealed gap.

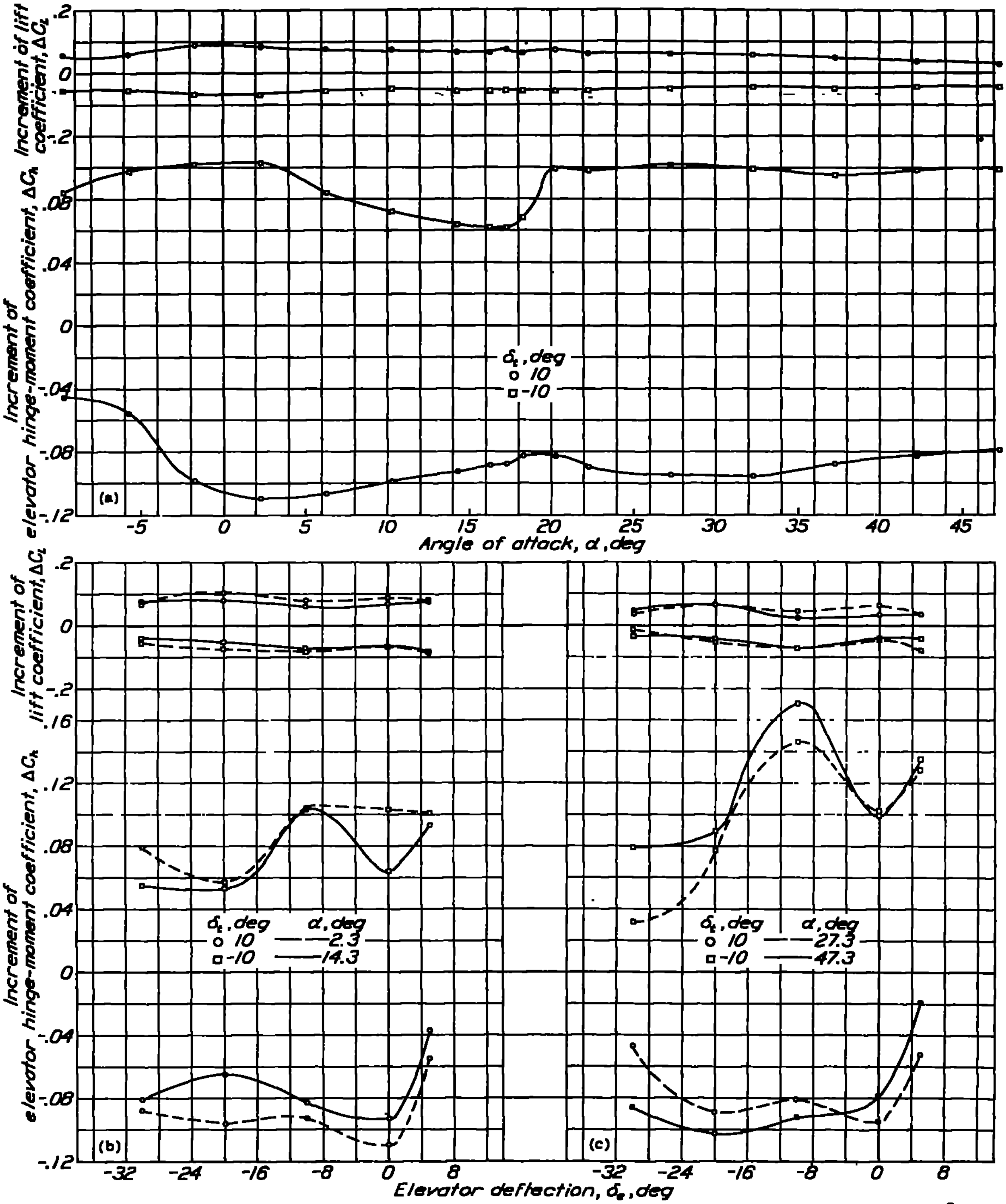

(a) ψ = 0°, δ_e = 0°. (b) α = 2.3° and 14.3°. (c) α = 27.3° and 47.3°.

Figure 14.- Increments of lift and elevator hinge-moment coefficients due to tab deflection as functions of both angle of attack and elevator deflection. A $0.20c_e$ tab on a plain elevator with sealed gap.

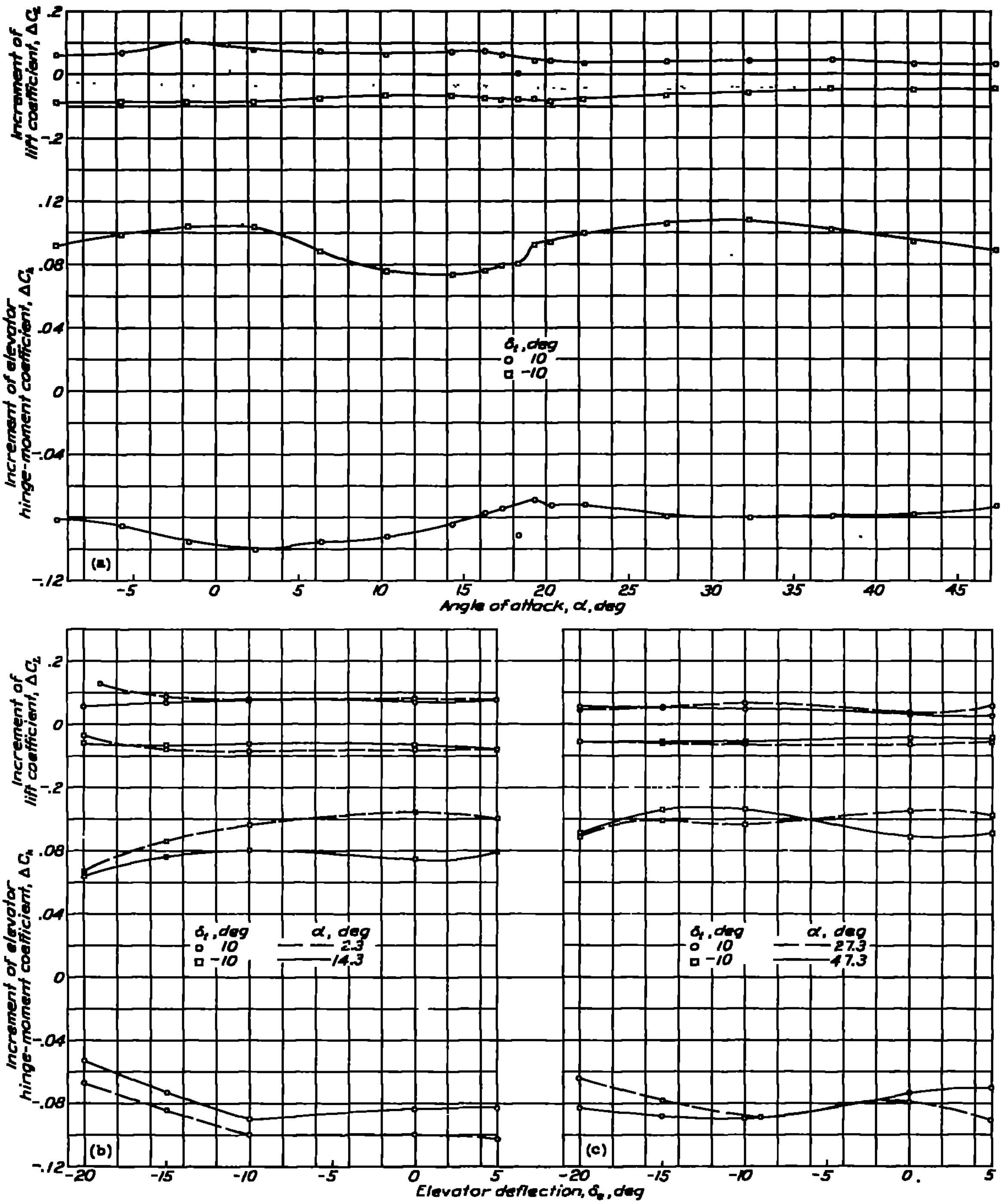

(a) $\psi = 0^\circ$, $\delta_e = 0^\circ$. (b) $\alpha = 2.3^\circ$ and 14.3°. (c) $\alpha = 27.3^\circ$ and 47.3°.

Figure 15.- Increments of lift and elevator hinge-moment coefficients due to tab deflection as functions of both angle of attack and elevator deflection. A $0.20c_e$ tab on an elevator with $0.75c_e$ blunt nose overhang and sealed gap.

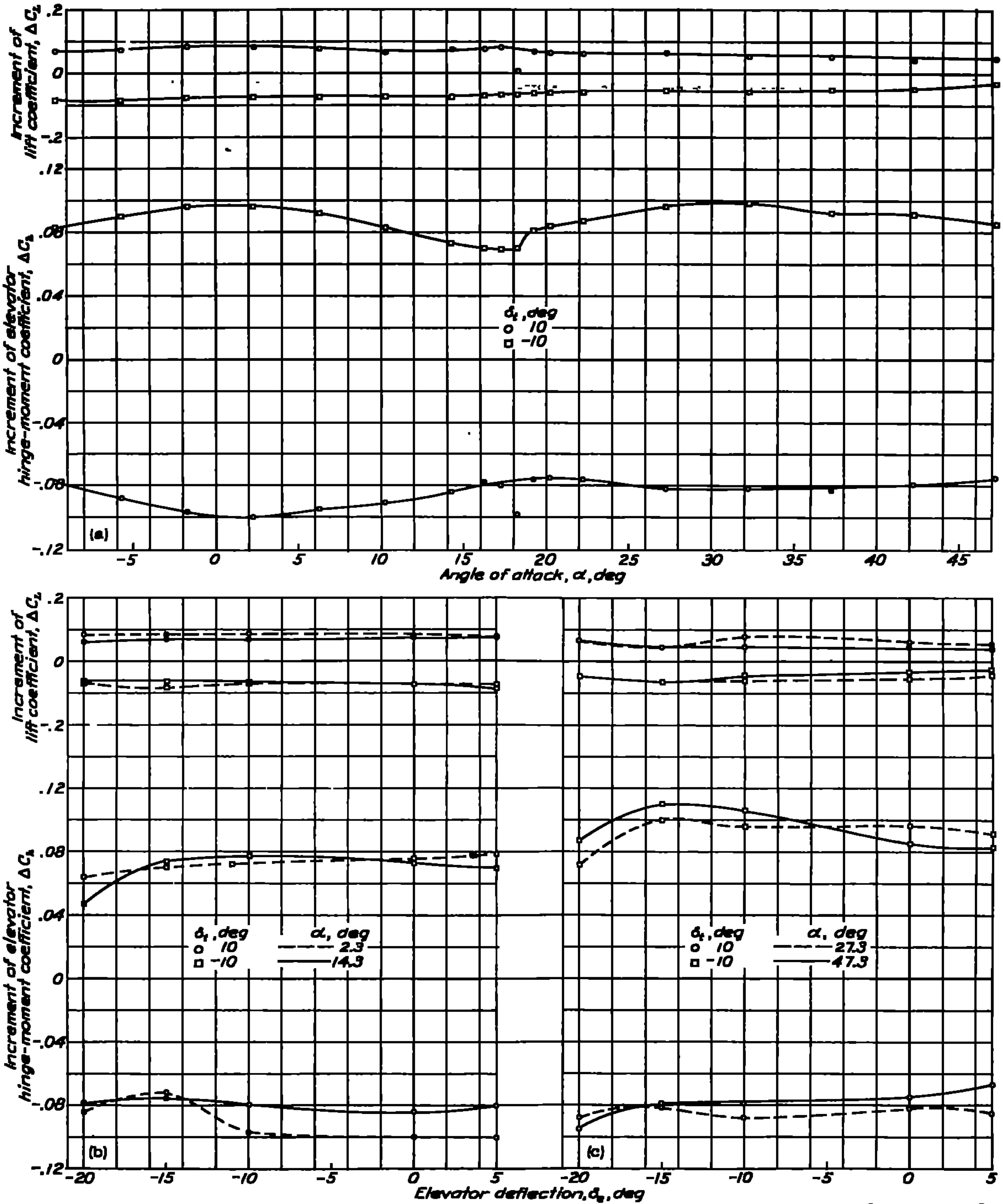

(a) $\psi = 0^\circ$, $\delta_e = 0^\circ$. (b) $\alpha = 2.3^\circ$ and 14.3°. (c) $\alpha = 27.3^\circ$ and 47.3°.

Figure 16.- Increments of lift and elevator hinge-moment coefficients due to tab deflection as functions of both angle of attack and elevator deflection. A $0.20c_e$ tab on an elevator with $0.75c_e$ sharp nose overhang and sealed gap.

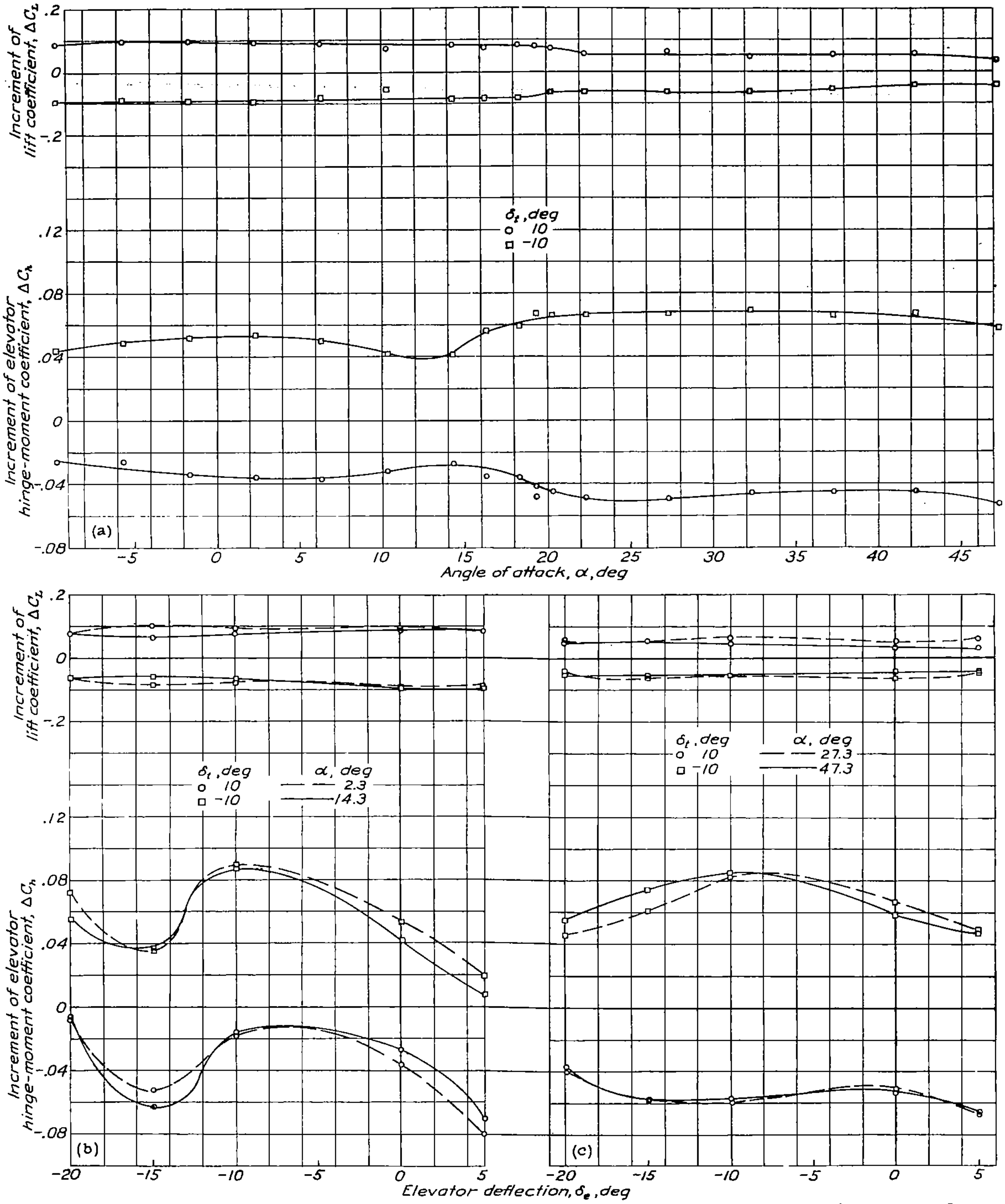

(a) $\psi = 0^\circ$, $\delta_e = 0^\circ$. (b) $\alpha = 2.3^\circ$ and 14.3°. (c) $\alpha = 27.3^\circ$ and 47.3°.

Figure 17.- Increments of lift and elevator hinge-moment coefficients due to tab deflection as functions of both angle of attack and elevator deflection. A $0.20c_e$ tab on elevator with $0.50c_e$ blunt nose overhang and sealed gap.

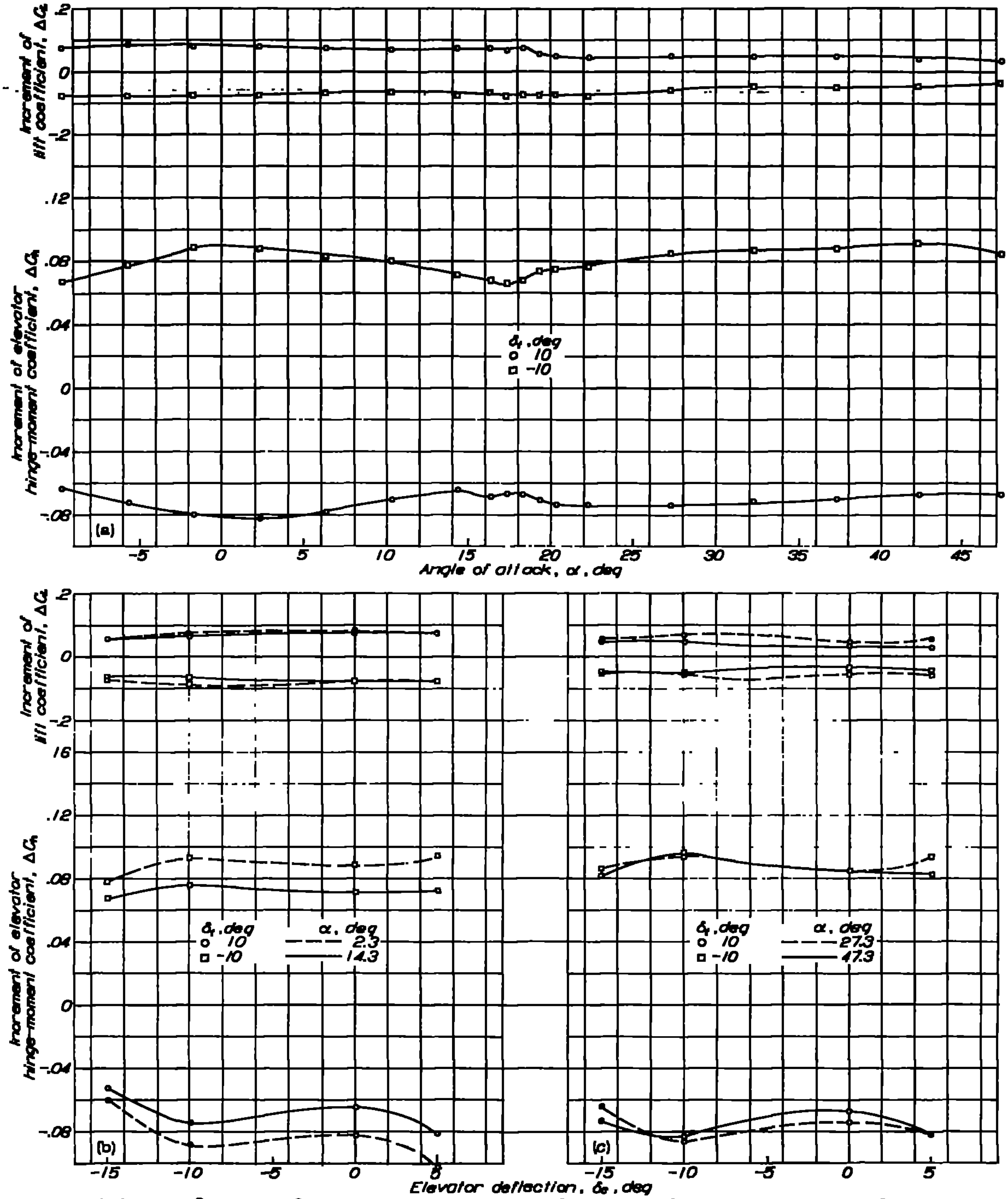

(a) $\psi = 0^\circ$, $\delta_e = 0^\circ$. (b) $\alpha = 2.3^\circ$ and 14.3°. (c) $\alpha = 27.3^\circ$ and 47.3°.

Figure 18.- Increments of lift and elevator hinge-moment coefficients due to tab deflection as functions of both angle of attack and elevator deflection. A $0.20c_e$ tab on an elevator with $0.50c_e$ sharp nose overhang and sealed gap.

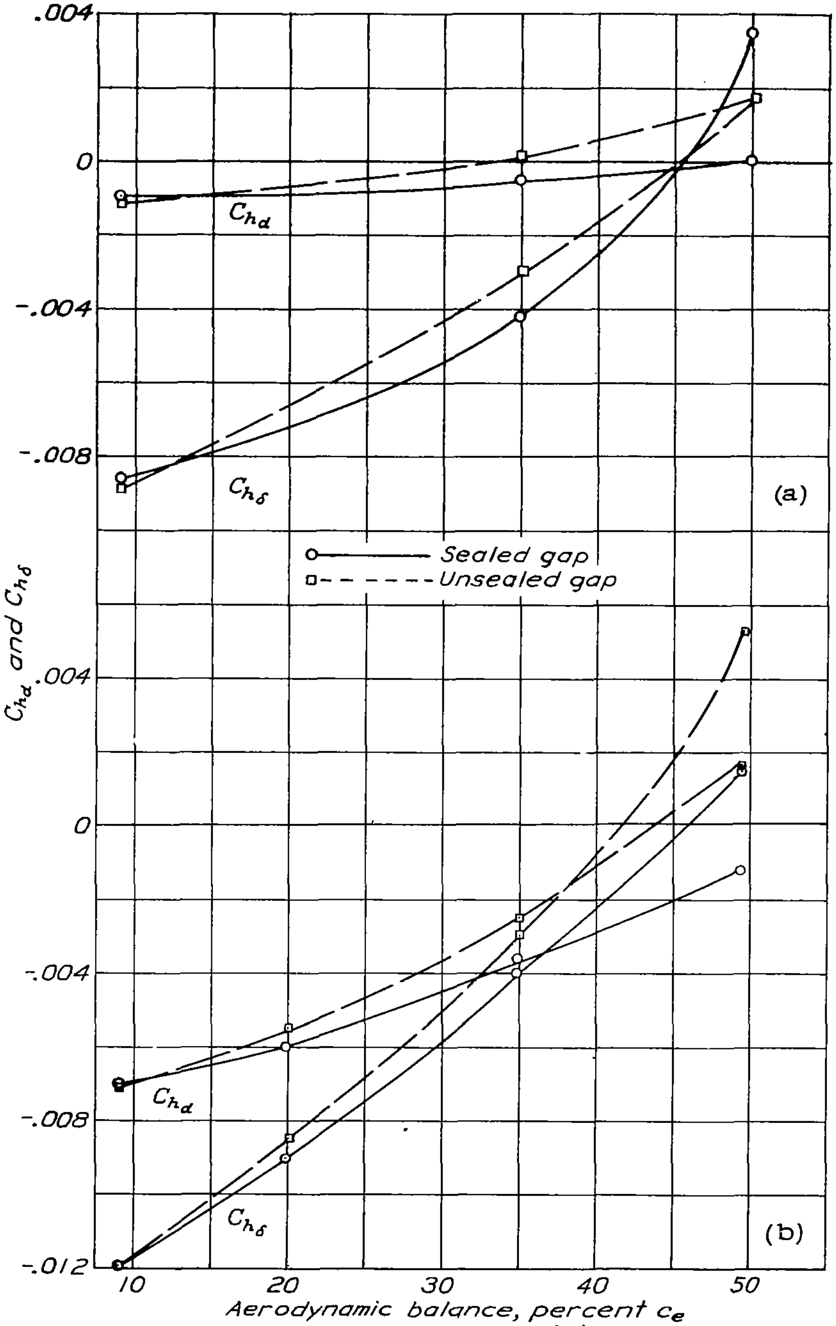

(a) Values from present tests. Elevator, 0.27c; A,3.8.

(b) Values from references 2,3,4 and 5. Elevator, 0.30c; A, ∞.

Figure 19(a,b).-Variation of hinge-moment parameters with aerodynamic balance as measured in both two-and three-dimensional flow. Blunt-nose balance.